

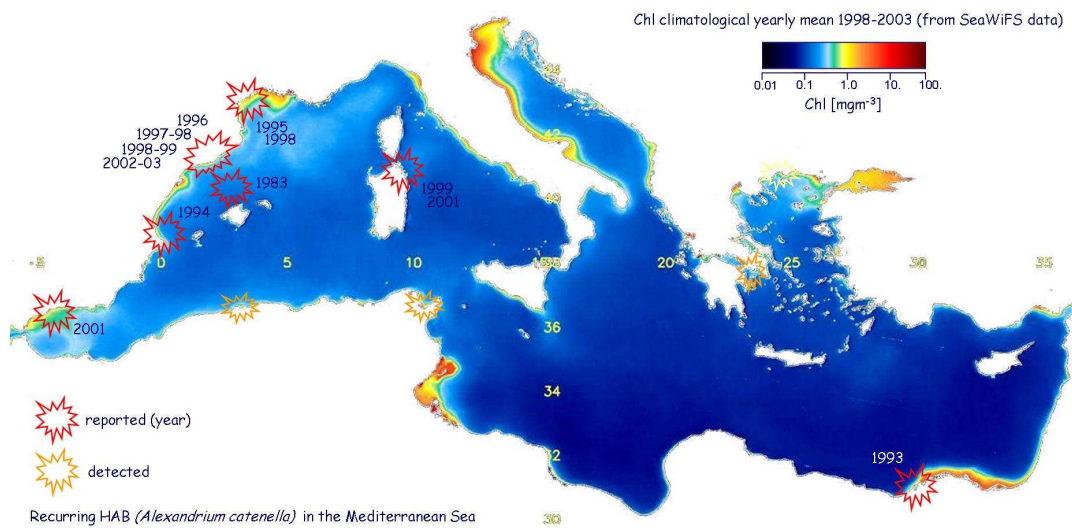


**EUROPEAN COMMISSION**  
DIRECTORATE-GENERAL  
**Joint Research Centre**

# *Bio-Optical Environmental Assessment of Marginal Seas*

## Progress Report 2

V. Barale <sup>(1)</sup>, J.M. Jaquet <sup>(2)</sup>, K. Allenbach<sup>(2)</sup>, M. Ndiaye<sup>(2)</sup>, A. Hoareau<sup>(2)</sup>



<sup>(1)</sup> Institute for Environment and Sustainability  
Joint Research Centre

<sup>(2)</sup> University of Geneva  
Earth Sciences Section, Remote Sensing and GIS Unit

Collaboration Agreement N° 21698-2004-02 SOSC ISP CH

## **LEGAL NOTICE**

Neither the European Commission nor any person acting of behalf of the Commission is responsible for the use which might be made of the following information.

A great deal of additional information on the European Union is available on the Internet. It can be accessed through the Europa server (<http://europa.eu.int>)

EUR 21899 EN  
© European Communities, 2005  
Reproduction is authorized provided the source is acknowledged  
*Printed in Italy*

## **Preface**

The research described in the present report has been undertaken in the frame of Collaboration Agreement N. 21698-2004-02 SOSC ISP CH between the Institute for Environment and Sustainability (IES), Joint Research Centre (JRC) of the European Commission (EC), and the University of Geneva, Section of Earth Sciences, Remote Sensing and GIS Unit. The joint activities on Bio-optical Environmental Assessments of Marginal Seas were conducted at the IES, JRC EC, within the FP6 Action 2121 ECOMAR, and at the University of Geneva, as part of the internship work program of Ms Karin Allenbach, Mr Maphathé Ndiaye and Ms Anaïs Hoareau, whose contribution to the results obtained by this study is gratefully acknowledged. The authors are greatly indebted to Dr Frédéric Melin, IES, JRC EC, for his stewardship in the production, maintenance and provision of SeaWiFS data.

## **Abstract**

Algal blooming in the Mediterranean Sea has been studied with an analysis of SeaWiFS-derived (1998-2003) *chl* anomalies and special features. Statistics of the anomalies, as well as comparisons with data collected *in situ*, were used to address the relationship between local and regional phytoplankton dynamics, in both the mesotrophic (sometimes eutrophic) western basin and the oligotrophic eastern basin. Intense coastal blooming appeared to be linked to local factors, and only occasionally connected to mesoscale features such as eddies or current meanders, suggesting that the forcing functions of local (harmful) algal blooms and regional blooms are different, or overlap only marginally.

## **Authors**

Dr Vittorio Barale  
Institute for Environment and Sustainability  
Joint Research Centre of the European Commission  
Via E. Fermi s.n. (tp 272), I-21020 Ispra (VA), Italy  
Tel +39 0332 789274 Fax +39 0332 789034  
e-mail: vittorio.barale@jrc.it

Dr Jean-Michel Jaquet  
Remote Sensing and GIS Unit, Earth Sciences Section, University of Geneva  
Rue des Maraichers 12, CH-1211 Genève, Switzerland  
Tel +41 22 379 6615  
e-mail: jean-michel.jaquet@terre.unige.ch  
and  
UNEP/DEWA/GRID, International Environment House  
11 Chemin des Anémones, CH-1219 Châtelaine, Switzerland  
e-mail : jean-michel.jaquet@grid.unep.ch

Ms Karin Allenbach, Mr Maphathé Ndiaye, Ms Anaïs Hoareau  
Remote Sensing and GIS Unit, Earth Sciences Section, University of Geneva  
Rue des Maraichers 12, CH-1211 Genève, Switzerland

## **Reference**

V. Barale, J.M. Jaquet, K. Allenbach, M. Ndiaye and A. Hoareau (2005). Bio-optical Environmental Assessments of Marginal Seas. Progress Report 2. European Commission, EUR 21899 EN, pp. 64.



# Table of Contents

	Foreword . . . . .	6
	Executive Summary . . . . .	7
1	Introduction . . . . .	9
1.1	Limitations of Optical RS Techniques . . . . .	9
1.2	The SeaWiFS-derived <i>chl</i> Database . . . . .	10
	<i>Plate 1. Statistical Aggregations, 1998-2003 chl Database . . .</i>	13
	<i>Plate 2. SeaWiFS-derived chl Climatological Yearly Mean . . . .</i>	14
	<i>Plate 3. SeaWiFS-derived chl Climatological Monthly Means . .</i>	15
	<i>Plate 4. SeaWiFS-derived chl yearly anomalies . . . . .</i>	16
	<i>Plate 5. GEBCO-derived mask for the Mediterranean Sea . . . .</i>	17
2	Blooming anomalies: a statistical approach . . . . .	19
	<i>Plate 6. SeaWiFS-derived chl monthly anomalies (2001) . . . . .</i>	21
	<i>Plate 7. Histograms of chl Anomaly Maps . . . . .</i>	22
	<i>Plate 8. Moran's I Time Variation, chl Monthly Anomalies . . . .</i>	23
	<i>Plate 9. Moran's I Correlogram and Fourier Spectrum . . . . .</i>	24
	<i>Plate 10. Fixed-point Time Evolution of chl Monthly Anomalies .</i>	25
	<i>Plate 11. Intercepts and Slopes, chl Anomaly Time Regression</i>	26
	<i>Plate 12.. Correlation Coefficients and Number of Samples . . .</i>	27
3	Algal Blooms in the South-Eastern Basin . . . . .	29
3.1	Spectral Signatures of <i>chl</i> Patters . . . . .	29
3.2	Comparing <i>chl</i> and <i>sst</i> Patterns . . . . .	30
	<i>Plate 13. SeaWiFS-derived chl, SE Basin, 2001 Daily Images</i>	32
	<i>Plate 14. SeaWiFS/MODIS-derived <math>L_{WN}</math>, Coastal Stations . . . .</i>	33
	<i>Plate 15. SeaWiFS-derived <math>L_{WN}</math> Spectra in Coastal Plumes . . .</i>	35
	<i>Plate 16. Profiles (EW and NS) of MODIS-derived chl and <i>sst</i> . .</i>	36
	<i>Plate 17. MODIS-derived chl and <i>sst</i> Patterns . . . . .</i>	37
4	Algal Blooms in the North-Western Basin . . . . .	39
4.1	Comparing Satellite and <i>in situ</i> Data Records . . . . .	39
	<i>Plate 18. Recurring HABs (Alexandrium Catenella), Med Sea . .</i>	42
	<i>Plate 19. SeaWiFS-derived chl, NW Basin, Monthly Means . . .</i>	43
	<i>Plate 20. SeaWiFS-derived chl (Catalonia), 2002 Daily Images</i>	44
	<i>Plate 21. SeaWiFS-derived chl (Catalonia), 2003 Daily Images</i>	45
	<i>Plate 22. SeaWiFS-derived chl (Sardinia), March 2002/2003 . .</i>	46
	<i>Plate 23. SeaWiFS-derived chl (Sicily), 2003 Daily Images . . . .</i>	47
5	Conclusion and Future Activities . . . . .	49
	References . . . . .	52
	Annex 1 <i>The Chlorophyll Auditor™ Software</i> . . . . .	55
	Annex 2 <i>The Alexandrium Genus in situ Data Record</i> . . . . .	57

## Foreword

Broad theme of the research program on “Bio-optical Environmental Assessments of Marginal Seas” is the exploitation of (optical) remote sensing data for the environmental assessment of the European Seas. The planned activities focus on the appraisal of recurring and/or anomalous phytoplankton growth patterns in enclosed seas – in the Mediterranean basin, in a first phase, and then possibly in the other continental basins – with implications ranging from water quality to climate issues. The final goal is to characterize eutrophic phenomena in surface waters, monitoring the concentration of chlorophyll-like pigments (*chl*), as appearing in the historical record of bio-optical satellite data, to develop an indicator of (harmful) algal blooms.

In the first phase of the present research program (see 1<sup>st</sup> Progress Report, Barale *et al.*, 2004), data collected by the Sea-viewing Wide Field-of-View Sensor (SeaWiFS), in the period 1998-2003, were used to explore the large-scale, long-term features of the chlorophyll-like pigment concentration (*chl*) field in the Mediterranean Sea. In order to understand the degree of background variability that could be found for this indicator, background variability on which anomalies could appear to be superimposed, the first issue approached was a trend analysis of the SeaWiFS data set at hand. Annual and monthly *chl* mean images, for all available years, were compared with the corresponding annual and monthly climatologies. Then, the anomalies determined by this comparison were discussed in terms of the oceanographic climate of the basin.

## Executive Summary

Algal blooming in the Mediterranean Sea has been studied with an analysis of SeaWiFS-derived (1998-2003) concentration of chlorophyll-like pigments (*chl*) anomalies and special features. Statistics of the monthly anomalies, as well as comparisons with *in situ* data, were used to address the relationship between local and regional phytoplankton dynamics, in both the oligotrophic eastern basin and the mesotrophic (or eutrophic) western basin.

The spatial structure of the anomalies has a non-random nature and varies periodically, over the annual cycle. The chronological evolution of the anomalies was studied by means of a pixel-by-pixel linear fit to the images. The resulting maps of intercept and slope are characterized by non-random patterns. Positive and negative values cluster in regions, indicating common evolution trends. The patterns are also somewhat correlated. Negative slopes, with positive intercepts, suggest that, between 1998 and 2003, anomalies have been getting smaller and smaller over most of the basin interior. This implies a general decrease in the blooming patterns, in good agreement with the decrease of the *chl* average basin value seen in the annual means. Positive slopes, with negative intercepts, suggest that anomalies have been getting larger and larger for a number of eddy-like structures in open waters, or extensive plumes in coastal zones.

The blooming hotspots, along the Catalan coast and the Egyptian-Israeli-Lebanese coast, present a number of similarities: large nutrient sources of continental origin; patterns of high water constituents concentrations, rooted at special coastal sites; strong current systems, inducing the offshore spreading of coastal plumes. Point sources of runoff are scattered along the coast; however, the main nutrient supply is upstream in the Levantine case (the Nile), downstream in the Catalan case (the Ebro). Further, the high-*chl* features off the south-eastern coast are larger, better recognizable against an oligotrophic background, while those off the north-western coast have smaller size and seldom merge with co-varying offshore patterns. The increasing positive trend of *chl* anomalies, appearing in both areas between 1998 and 2003 tallies with a growing “biological dynamism” at these sites (i.e. the expansion of coastal fisheries, in the south-east, and the intensification of noxious or harmful blooms in the north-west).

The filaments and plumes in the Levantine are linked to coastal runoff (and not to coastal upwelling, owing to a temperature higher than that of surrounding waters) and interact with large mesoscale dynamical features, such as offshore eddies or current meanders, typical of that part of the basin. The blooms along the Catalan coast appear to be confined to the near-coastal zone and separated from the offshore regional patterns, suggesting that the forcing functions of the two kinds of blooms are different, or overlap only marginally.





## 1. Introduction

Anomalous algal blooms – as well as a growing incidence of Harmful Algal Blooms (HAB) in unusual areas, like the Mediterranean Sea – are related to changes in the ecological balance of coastal and marine environments. A wealth of novel data on such changes comes from Remote Sensing (RS) from Earth orbit, which can support *in situ* measurements of phytoplankton dynamics with observations made over a wide range of space scales (*i.e.* from a few km to thousands of km) and of time scales (*i.e.* from days to years). In particular, optical RS allows basin-wide, multi-annual monitoring of algal bloom indicators such as the concentration of chlorophyll-like pigments, in the following referred to as *chl* (Barale, 1994, and references therein).

In the case study presented here, space and time blooming patterns in the Mediterranean Sea have been investigated by means of a data set collected by the Sea-viewing Wide Field-of-View Sensor (SeaWiFS), which started its multi-annual mission in September 1997 (Hooker *et al.*, 1992). Statistics of the *chl* indicator and its anomalies, as well as comparisons with analogous data collected either from space or *in situ*, were used to highlight “hotspots” for phytoplankton blooming in the basin, as well as to address the relationship between local and regional phytoplankton dynamics, in both the oligotrophic eastern basin and the mesotrophic, sometimes even eutrophic, western basin.

### 1.1 Limitations of Optical RS Techniques

If the assessment of *chl* in open waters can be accomplished with considerable accuracy, it must be recalled that several limitations still hamper the potential usefulness of optical RS, especially in near-coastal areas. This because of the complexity of separating the various contributions to the spectrum of visible light emerging from the sea surface – which may be due to diverse water constituents, or to the morphological setting of the area observed, or to the limitations of the remote sensors’ space/time resolution. Primarily, uncertainties can arise in the computation of *chl* absolute values, owing to the presence of optically active materials other than phytoplankton and related pigments (*i.e.* dissolved organic matter and suspended inorganic particles), with partially overlapping spectral signatures (Bukata *et al.*, 1995). Other factors, however, must also be accounted for.

Remote sensors working in the visible spectral range measure the amount of electromagnetic radiation – from which *chl* is later derived – coming from the ground footprint of each picture element (pixel, in brief) of an image, as an integrated value over a 3-dimensional water element, having dimensions given by the sensor spatial resolution (about 1.2 km × 1.2 km at nadir, for SeaWiFS) and the 1st optical depth (*i.e.* the depth at which solar irradiance falls to 1/e, or 0.37, of its value just below the surface; this depth, over which 90% of the

signal observed at the surface is originated, varies from tens of m, in clear oceanic waters, to a few m, or even cm, in turbid coastal waters, depending on the nature and concentration of water constituents). On one hand, the pixel-integrated *chl* value is hardly comparable with corresponding punctual measurements performed *in situ*. On the other, the same pixel-integrated value may have been computed with a spatial resolution (2 km across each scan line, after re-mapping, for SeaWiFS) too poor to distinguish individual near-coastal blooms, which can occur at scales well below the nominal pixel size.

Even if a relatively highly reflective target, such as a sub-pixel bloom, could be bright enough to affect the spectral signature of a whole picture element, it should be also considered that, in general, the pixels adjacent to the coast are composed by a mixed signal, coming from both the water side and the land side of the coastal interface, and this prevents the assessment of accurate *chl* values in those pixels. The impact of coastal reflectivity, or adjacency effect, can actually extend to several pixels, altering the accuracy of the retrieved signal for a considerable distance from the coast in the offshore direction. Basin morphology too has an impact on remote measurements. In shallow waters, direct reflection from the bottom, above the 1st optical depth, can provide a non-negligible contribution to the signal recorded by the sensor, leading to overestimate the real amount of phytoplankton present in the water column. In deep waters, conversely, the presence of an undetected deep chlorophyll *maximum*, below the 1st optical depth, can lead to an underestimate of the total amount of phytoplankton in the water column.

All these limitations suggest that the information on coastal blooms, obtainable from optical observations, should be restricted to spatial and temporal patterns and gradients, rather than absolute values, a fact that was kept in due account, when carrying out the present analysis of SeaWiFS imagery. However, when the limitations above are suitably accounted for, the analysis of historical times of satellite data can provide at least qualitative information on recurrent or anomalous algal blooms, and related environmental boundary conditions. In the following, after a brief description of the satellite data considered (and of the corresponding *in situ* measurements, when available; see Annex 1), an analysis will be presented of the SeaWiFS-derived *chl* data, their anomalies and association with other environmental features. Further, the report will explore the possible links of near-coastal blooms to either local forcing factors or to the impact of pelagic conditions.

## **1.2 The SeaWiFS-derived *chl* Database**

The satellite data record considered to examine the evolution of *chl* in the Mediterranean Sea, generated by the SeaWiFS from 1998 to 2003, comprises a time series of individual daily images, collected when favorable meteorological conditions occurred over (at least part of) the

European continent and seas. In those cases when two images of the same area were collected by the sensor in the same day, due to the overlap of two consecutive orbits at high latitudes, only one value per pixel was retained in the processing chain (*i.e.* the value from the scene for which that pixel was observed with the lowest viewing angle). Each of the available images was treated on a pixel-by-pixel basis, to correct top-of-the-atmosphere radiances from atmospheric noise, to derive normalized water-leaving radiances  $L_{WN}$  and then to compute the concentration of water constituents (including *chl*) from the obtained water-leaving radiances. The original data were processed using the SeaDAS algorithm set (Fu *et al.*, 1998), with additional modifications described in Melin *et al.* (2000) and in Sturm and Zibordi (2002). Individual *chl* daily images, covering sections of the Mediterranean area, were further re-mapped on a common equal-area (Alber's) projection grid, degrading the original 1.2 km nominal resolution (at nadir) to a uniform 2 km. Image edges, where pixel resolution exceeds 2 km, were excluded from the re-mapping.

Starting from the daily *chl* maps, a series of statistical aggregations was derived for the entire 1998-2003 period (see Plate 1). Composite *chl* fields, at the yearly and monthly scales, were derived from the re-mapped images by simple time averaging. Climatologies at the yearly and monthly scales were computed as means of all composite images available for each period. Further, *chl* anomalies, again at the yearly and monthly scales, were computed as the difference between each yearly mean and the climatological year, and between each monthly mean and the corresponding climatological month, respectively.

In general, the yearly climatological mean (Plate 2) shows a wide range of *chl* values, which appear to be about one order of magnitude lower in the south-eastern part of the basin than in the north-western part. The monthly climatological means (Plate 3), composing the yearly mean, show that most of the high *chl* events observed offshore are shaped by interacting mesoscale structures such as pelagic eddies and meanders. The observable inshore events appear to co-vary with the offshore patterns, but to develop primarily as independent features along the innermost coastal area. When these near-coastal features do interact with the larger basin-wide patterns, they seem to do so extending seaward from to coast, and not to develop under the impact of phenomena taking place in open waters.

The *chl* anomaly maps (see *e.g.* the yearly anomalies series in Plate 4) highlight the geographical spread and intensity of blooming patterns, which differed in each period from the corresponding climatological mean. The series shows that anomalies can occur anywhere in the basin, even though they tend to recur in areas of intense blooming, and in all periods of the year. There are at least three general types of anomalies, which seem to be of particular interest. The first is a basin-wide anomaly, when the whole Mediterranean basin appears to be

above or below the climatological mean value (see *e.g.* the 2000 anomaly map, in plate 4). The second kind of anomaly shows the western and the eastern basins oscillating in opposite ways, one above and one below the climatological mean value (see *e.g.* the 2001 anomaly map, in plate 4). In general, though, the most common anomalies are of a third kind, which involves only a specific sub-basin or near-coastal area (see *e.g.* the 1998-1999 as well as the 2002-2003 anomaly maps, in plate 4). In the western basin, the Alboran Gyres – Algerian Current system and more prominently the Ligurian-Provençal Sea, where the most intense blooming occurs, are the main sites of these recurring local anomalies. In the eastern basin, the gyre system south-east of the Island of Crete and, somewhat surprisingly, the Egyptian-Israeli-Lebanese coastal area display similar features.

The observations above have been examined and discussed, mostly by visual inspection – and a number of hypotheses suggested – in Barale *et al.* (2004). The work presented here focuses onto a statistical approach to the analysis of the *chl* (monthly) anomalies. To this end, data from the Mediterranean proper were extracted from the anomaly maps, discarding pixels from other water bodies as well as shallow-water coastal pixels. Following earlier studies on the influence of bottom reflectance on the chlorophyll signal (Jaquet *et al.*, 1999), pixels with a depth equal or shallower than 30 m were eliminated by means of a mask derived from the General Bathymetric Chart of the Oceans (GEBCO) data set<sup>1</sup>, suitably geo-referenced to the same *chl* maps projection (Plate 5, panel 1). The resulting monthly anomaly (reduced) maps were further analyzed, in order to (i) quality-check the data (for distribution type, outliers, “anomalies” within the anomalies, *etc.*), and to evaluate (ii) spatial structures and (iii) temporal trends, using first a pixel-by-pixel linear fit in time and then mapping on the same geographical grid intercepts and slopes, as well as correlation coefficients and number of samples, obtained for each pixel.

Finally, two specific areas, in the south-eastern and the north-western Mediterranean Sea, which emerged as outstanding hotspots for algal blooming, were considered for more in depth analyses (Plate 5, panels 2 and 3). *Ad hoc* time series of (*quasi*) cloud-free images were selected in the summers of 2001 and 2002 for the Egyptian-Israeli-Lebanese coastal areas (60 and 25 images, from June to August, respectively), and year-round in 2002 and 2003 for the Catalan Coast (90 and 96 images, respectively), together with the islands of Sardinia (93 and 91 images, respectively) and of Sicily (95 images, in both years). These series were compared with optical and thermal data collected by other orbital sensors (*i.e.* the Moderate Resolution Imaging Spectrometer, MODIS, and the Advanced Very High Resolution Radiometer, AVHRR) and with *in situ* data on recurring HAB episodes.

---

<sup>1</sup> <http://www.ngdc.noaa.gov/mgg/gebco/grid/1mingrid.html>

*Plate 1. Statistical Aggregations for the 1998-2003 chl Database*

---

no.	data products	identifiers
6	Yearly Means	$YM_n$ <span style="float: right;">n=1,6</span>
1	Climatological Yearly Mean	CYM
6	Yearly Anomalies	$YA_n = YM_n - CYM$
72	Monthly Means	$MM_{nm}$ <span style="float: right;">m=1,12</span>
12	Climatological Monthly Means	$CMM_m$
72	Monthly Anomalies	$MA_{nm} = MM_{nm} - CMM_m$

Plate 2. SeaWiFS-derived chl Climatological Yearly Mean

---

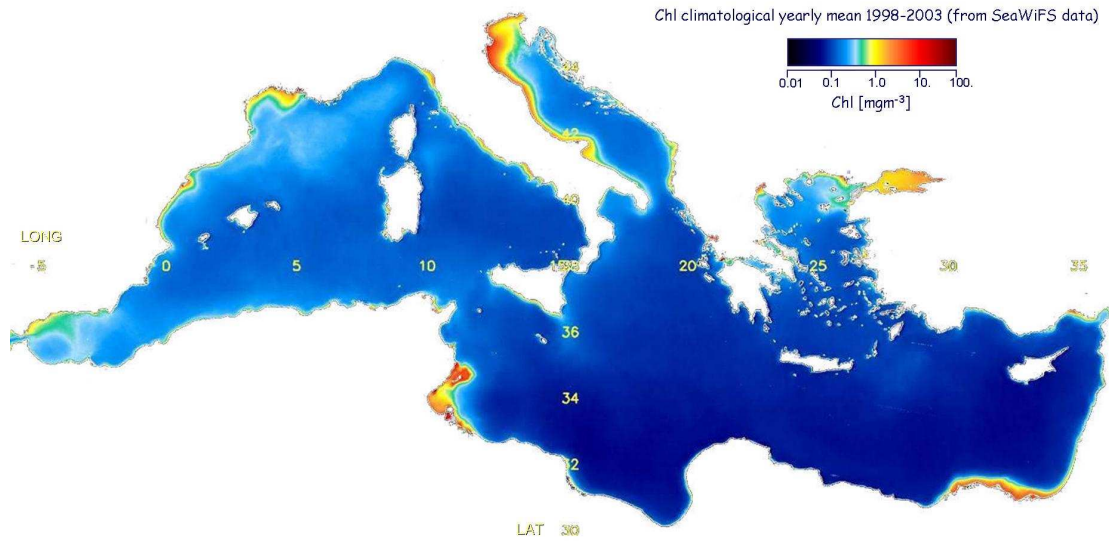
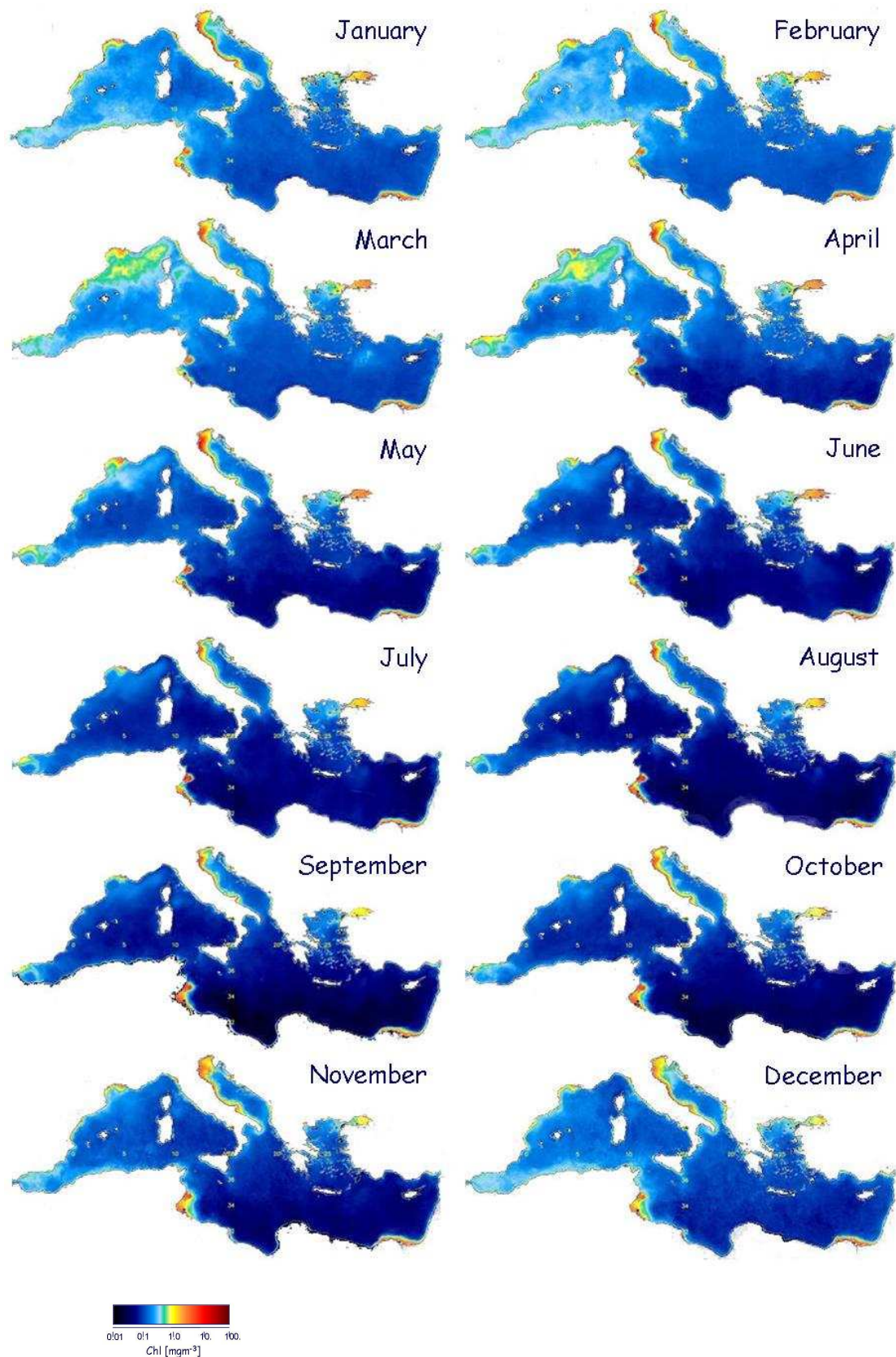


Plate 3. SeaWiFS-derived chl Climatological Monthly Means

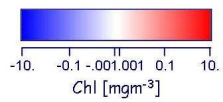
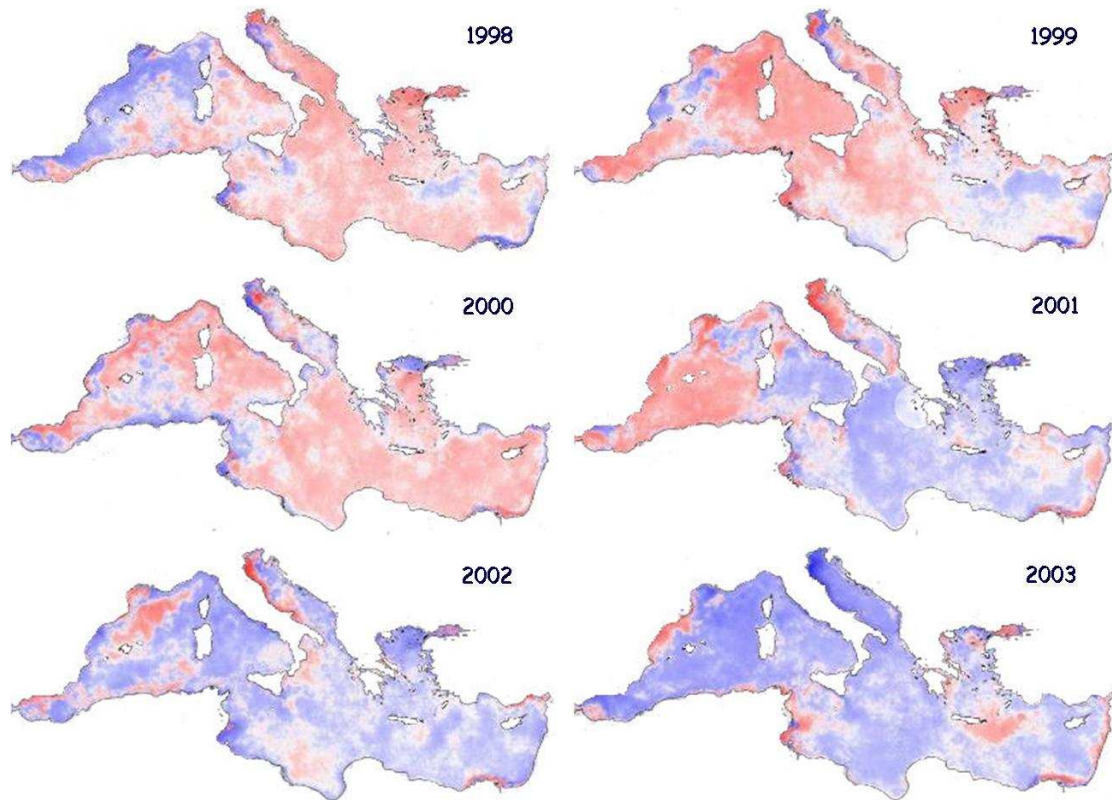


Chl climatological yearly mean 1998-2003 (from SeaWiFS data)



Plate 4. SeaWiFS-derived chl yearly anomalies

---

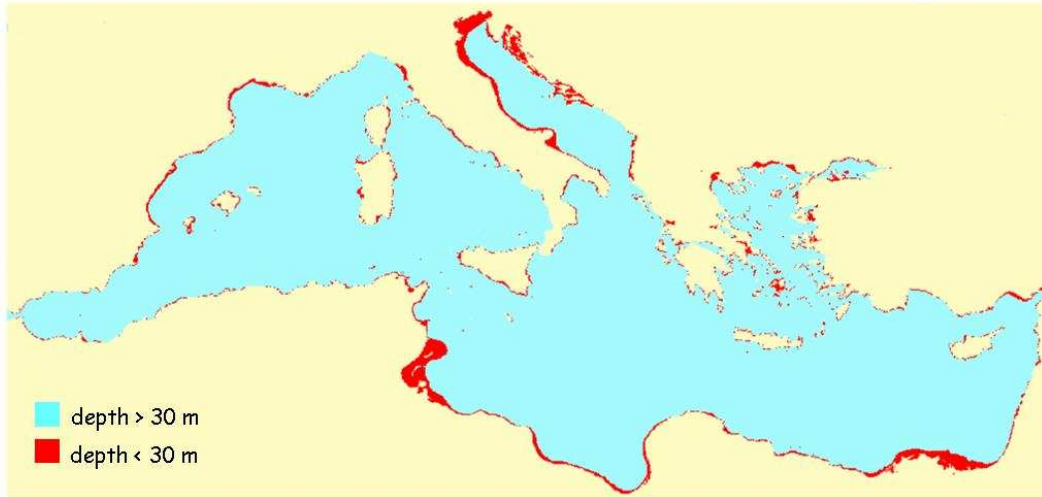


Chl yearly anomalies 1998-2003 (from SeaWiFS data)



Plate 5. GEBCO-derived mask for the Mediterranean Sea

---



Panel 1. GEBCO-derived bathymetry mask (in red) for the Mediterranean Sea.



Panel 2. Detail for the NW coastal area.



Panel 3. Detail for the SE coastal area.



## 2. Blooming anomalies: a statistical approach

A statistical analysis of blooming anomalies was carried out (by means of *ad hoc* software produced for the present study; see Annex 1) using the set of  $12 \times 6 = 72$  *chl* monthly anomaly reduced maps, obtained by subtracting the matching climatological monthly mean from each *chl* monthly mean image of the period 1998-2003. An example of the 12 *chl* monthly anomaly reduced maps for 2001 is shown in Plate 6.

The statistical distributions of the *chl* monthly anomalies are characterized by a wide dispersion, which hampers somewhat the representation of their histograms (see *e.g.* Plate 7, panel 1). A more useful display can be obtained by a limitation to the 97.5% confidence interval (Plate 7, panel 2). The examination of the 72 histograms shows a variety of distributions, either symmetrical (Plate 7, panel 2) with varying degrees of peakedness, or skewed (Plate 7, panel 3), or polymodal (Plate 7, panel 4).

As an initial step, the spatial structure of the monthly anomalies was assessed by means of Moran's *I* coefficients (Moran, 1950), a measure of the overall lag-one auto-correlation, with limits of  $-1 \leq I \leq +1$  and a minimum value of 0 for a totally uncorrelated regionalized (random) variable. A sequence of one single value of the coefficient *per* monthly anomaly was computed, and then plotted against time, so as to provide the time series of coefficients shown in Plate 8. Apart from an abnormally low value in December 1998 (abnormal, but not inconsistent with the systematic December *minima*), the auto-correlation varies between 0.6 and 0.9, indicating a non-random nature of the series' variability. The variations also seem to be definitively periodic. This hypothesis was tested by computing the correlogram of the time series, as well as its Fourier spectrum (Plate 9). On both diagrams, there is a significant major peak at a frequency close to 12 months. As shown by Moran's *I* coefficients, the spatial structure of the anomalies varies periodically, over the annual cycle, with higher values in summer than in winter.

The chronological evolution of the monthly anomalies was studied by means of a pixel-by-pixel linear fit to the images, and then by considering slopes, intercepts, correlation coefficients and number of samples (used to compute the significance level of the correlation coefficient). Prior to the computation, monthly anomalies expressed in absolute values ( $\text{mg m}^{-3}$ ) were converted in % values, in order to enhance existing trends even in the case of weaker anomalies. Plate 10 shows an example of the regressions which have been computed on each of the 1,653,340 pixels composing the (reduced) maps. The trend parameters obtained (*i.e.* intercept, slope, correlation coefficient, number of samples) were mapped again on the same geographical grid. Both intercept and slope can be either positive or negative.

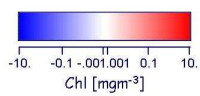
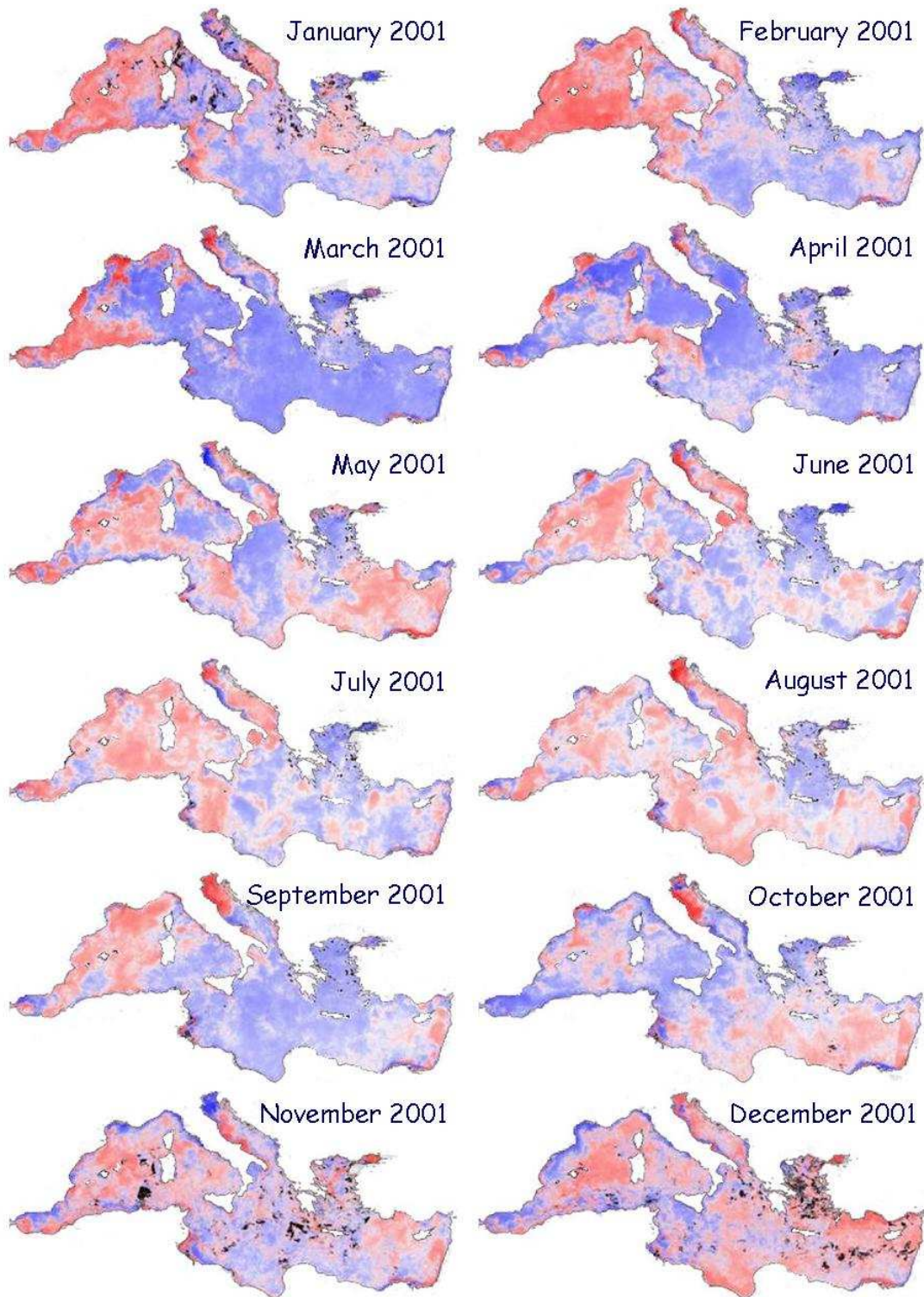
The intercept and slope values, shown in Plate 11, are characterized by non-random patterns. In spite of some noise, positive and negative values cluster in regions, indicating common evolution trends. Intercept and slope patterns are somewhat correlated across both maps: negative intercepts mostly coincide with positive slopes (see *e.g.* the Alboran Sea as well as the Balearic-Provençal-Ligurian Sea, in the western basin; the north-western Adriatic Sea and the north-eastern Aegean sea; the areas south and east of Crete as well as offshore the Egyptian-Israeli-Lebanese coast, in the eastern basin) and vice-versa.

The significance of the intercept and slope patterns can be derived from the maps of the correlation coefficients  $r$  and number of samples  $n$  shown in Plate 12. From the latter, it can be seen that  $n$  is predominantly higher than 65. For this value of  $n$ , the 95% significance level for  $r$  is 0.25 (0.32 for 99%). Hence, based on the map in Plate 12, intercept and slope trends are significant in the areas where  $r$  is color-coded as mid-to-dark blue and mid-to-dark red.

Most of the Mediterranean area shows negative slopes, with positive intercepts, suggesting that, between 1998 and 2003, anomalies have been getting smaller and smaller over the largest part of the basin interior. Some small areas with negative slopes even show negative intercepts, as in the marginal easternmost area of the Ligurian-Provençal Sea. Given that the regressions concern % anomalies, this would imply a general decreasing variability in the blooming patterns, in good agreement with the general decrease of the *chl* average basin value already seen in the annual means (Barale *et al.*, 2004).

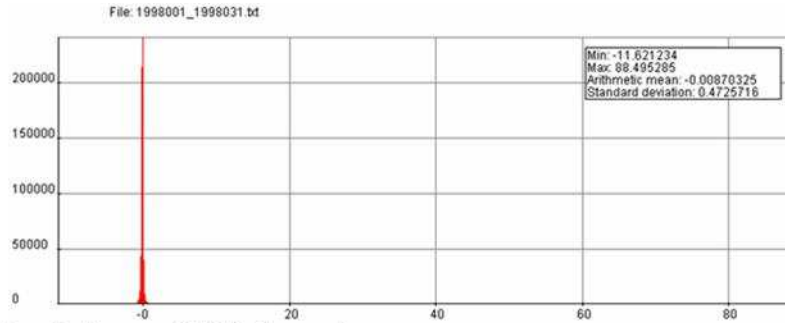
Other areas show a counter-trend of positive slopes, with negative intercepts, presenting eddy-like structures in open waters (*e.g.* in the Gulf of Lions and along the Algerian current, in the west; around the Rhodes Gyre, in the east), or extensive coastal plumes (*e.g.* along the Catalan coast and the Egyptian-Israeli-Lebanese coast). In the Gulf of Lions, the *chl* anomalies have been mostly negative, following winters in which the so-called “blue hole” (Barale *et al.*, 2004) – indicative of strong deep convection processes – did not develop or appeared to be weaker. Instead, increasingly positive anomalies characterized the greater part of the period, in which strong vertical mixing, with consequent enrichment of the surface layer by deep nutrients, left a clear mark first in a well developed “blue hole” and then in the extensive blooming patterns. Finally, in the coastal regions of both the north-west and the south-east, it appears that anomalies have been getting larger and larger, in the period considered – in parallel to recurrent blooms of alien (noxious or harmful) phytoplankton species or to improving local fisheries, respectively (see following chapters). These particular areas, true “hotspots” for anomalous algal blooming, have been examined in some detail, to try and understand (at least from a qualitative point of view) the relationship between blooms and local *vs* regional environmental factors.

Plate 6. SeaWiFS-derived chl monthly anomalies (2001)

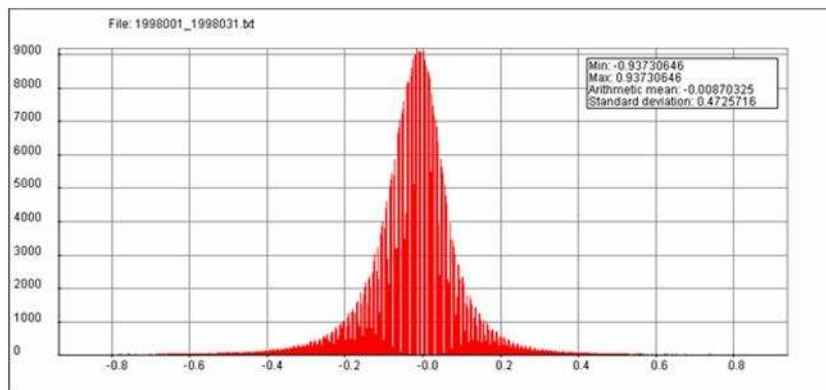


Chl yearly anomalies 1998-2003 (from SeaWiFS data)

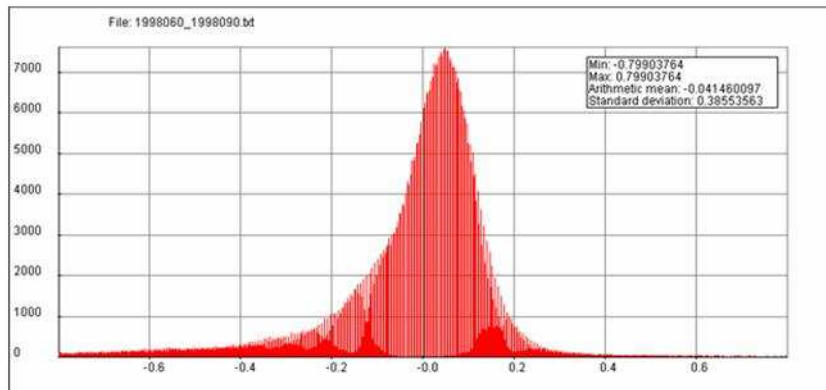
Plate 7. Histograms of chl Anomaly Maps



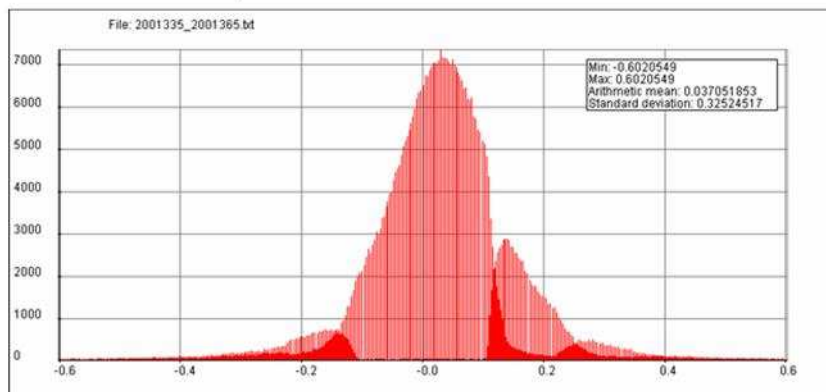
Panel 1. January 1998. Full spread.



Panel 2. January 1998. Spread limited to  $\pm 97.5\%$  confidence interval. Symmetrical.



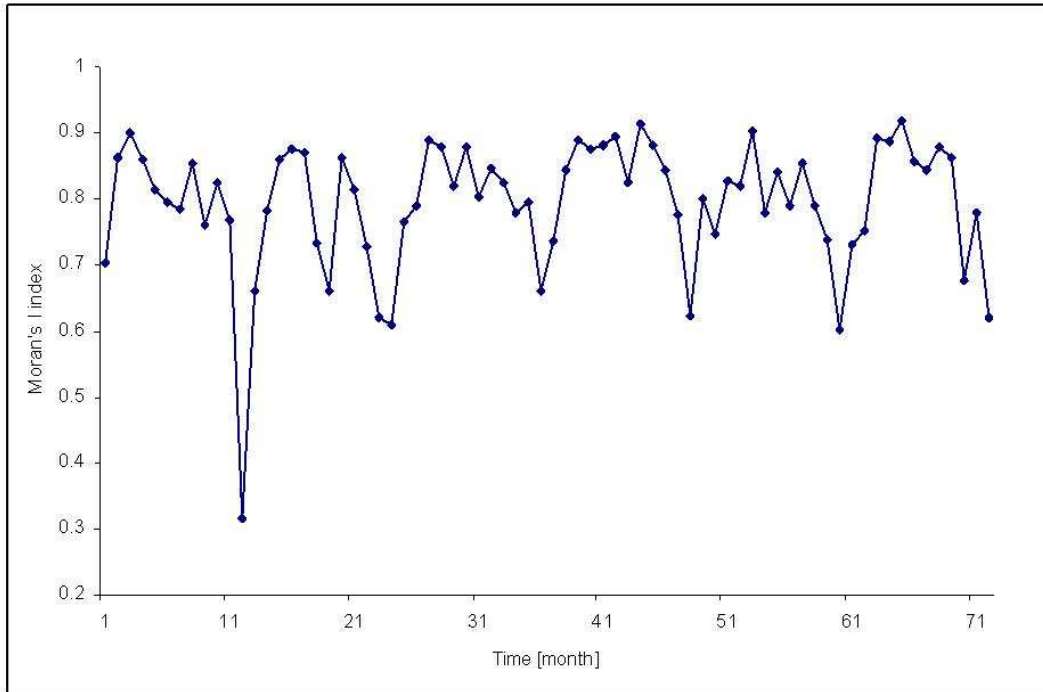
Panel 3. March 1998. Spread limited to  $\pm 97.5\%$  confidence interval. Skewed.



Panel 4. December 2001. Spread limited to  $\pm 97.5\%$  confidence interval. Polymodal.

Plate 8. Moran's I Time Variation, chl Monthly Anomalies (1998-2003)

---

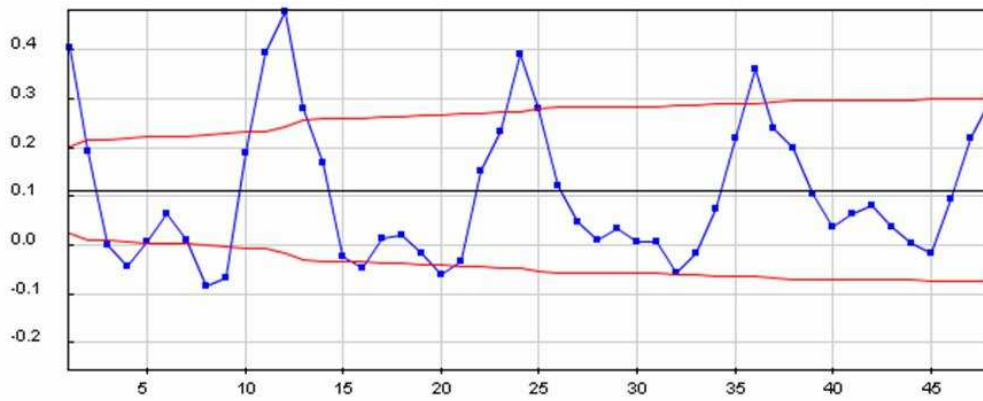


Variation in time of Moran's I coefficients computed for the chl monthly anomalies (98-03)

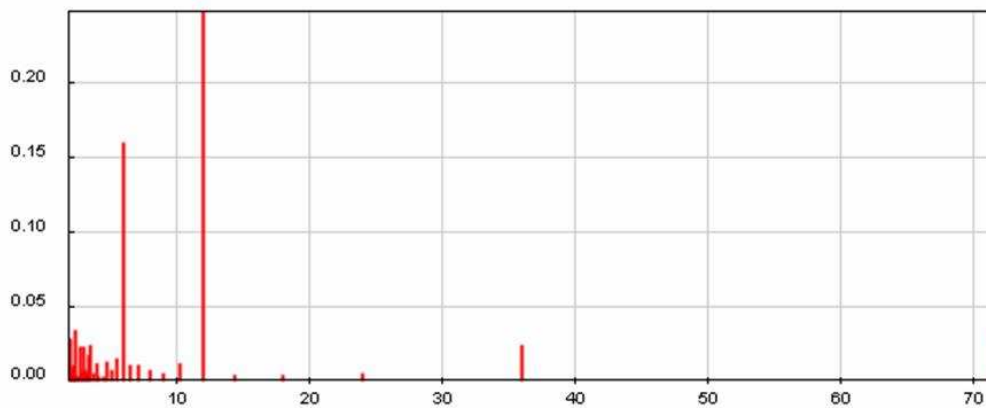


Plate 9. Moran's I Correlogram and Fourier Spectrum

---



Correlogram of Moran's I coefficients (in blue) computed for the chl monthly anomalies (98-03) 95% confidence interval in red.

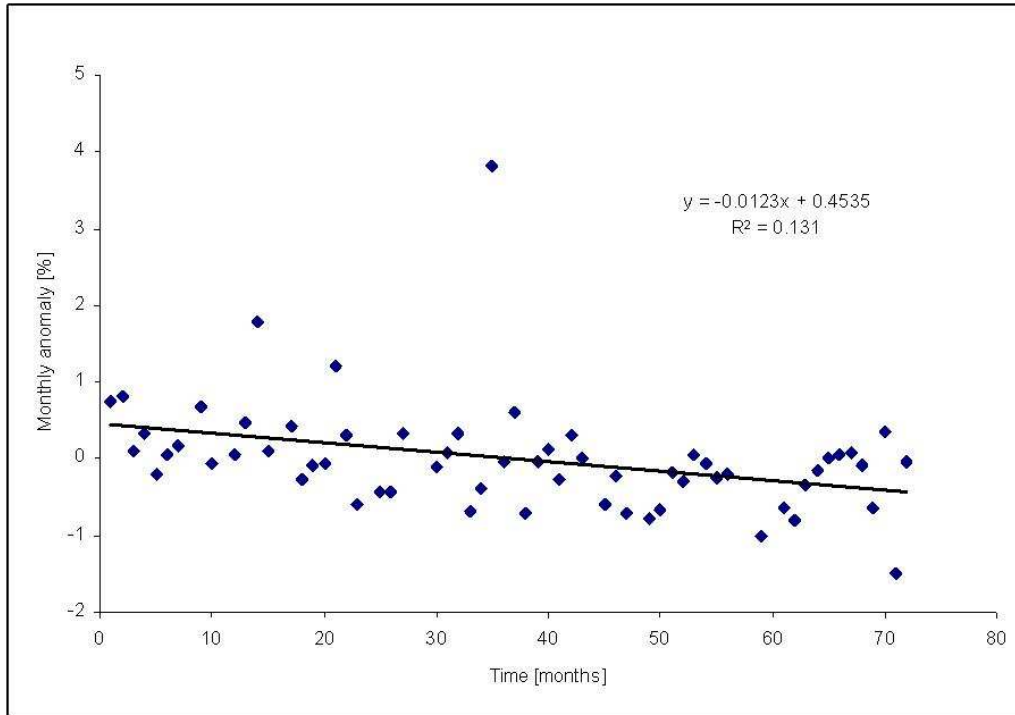


Fourier spectrum of Moran's I coefficients computed for the chl monthly anomalies.



Plate 10. Fixed-point Time Evolution of chl Monthly Anomalies

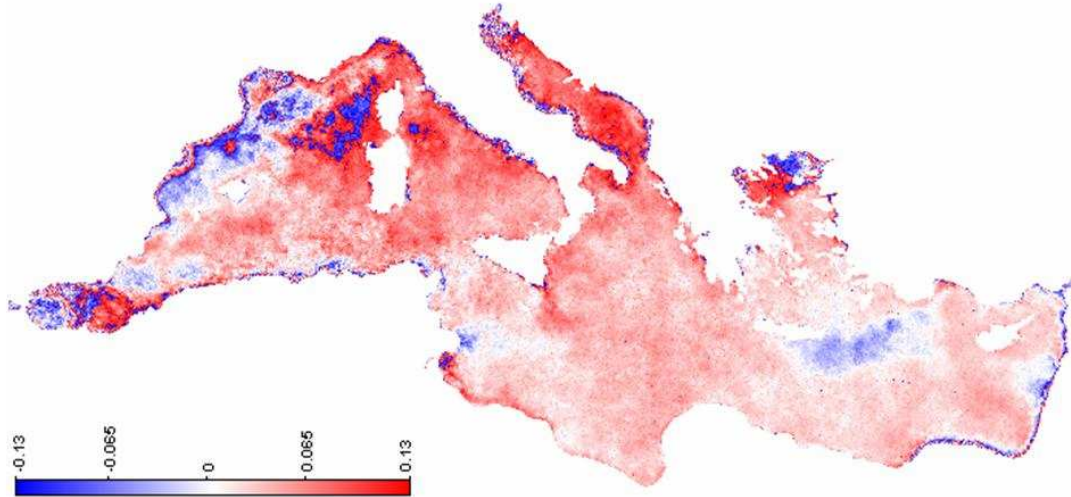
---



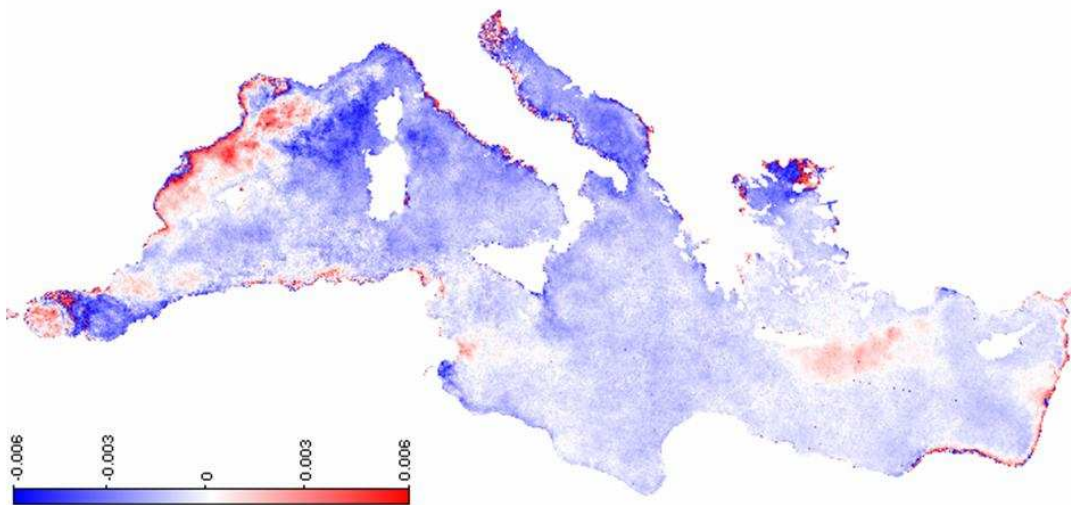
Chronological evolution of the chl monthly anomalies, converted in % values, at a given point of the Med geographical grid, with corresponding linear regression. Note the presence of an outlier.

*Plate 11. Intercepts and Slopes, chl Anomaly Time Regression*

---



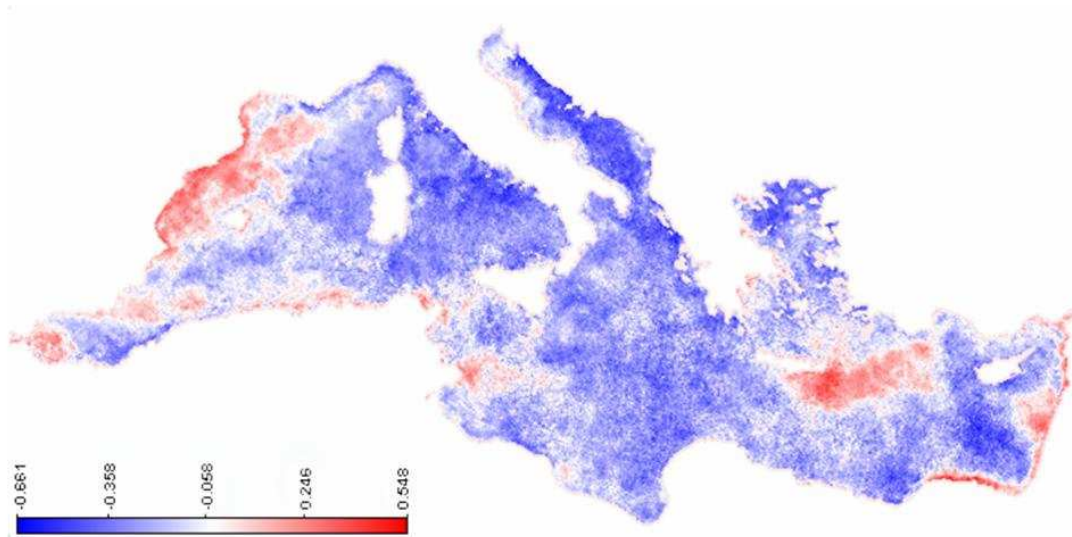
INTERCEPT values for the time regression of the chl monthly anomalies (98-03) in %.



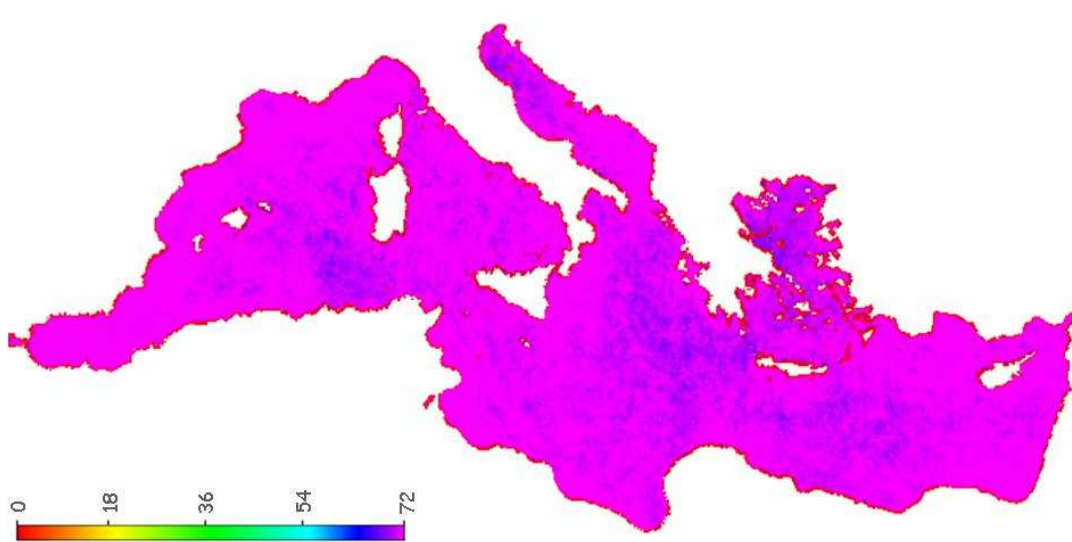
SLOPE values for the time regression of the chl monthly anomalies (98-03) in %.

Plate 12. Correlation Coefficients and Number of Samples

---



CORRELATION COEFFICIENT values for the time regression of the chl monthly anomalies (98-03) in %.



NUMBER OF SAMPLES for the time regression of the chl monthly anomalies (98-03) in %.



### **3. Algal Blooms in the South-Eastern Basin**

Whereas the Levantine Basin of the Mediterranean Sea is known for its generally oligotrophic character, sizeable high-*chl* filaments and plumes originating from the Egyptian-Israeli-Lebanese coastal area are evident in the SeaWiFS data set (Weber *et al.*, 2004; see *e.g.* the image series of Plate 13). The river Nile plume is by far the main (near-coastal) feature of the south-eastern basin, and provides a constant source of nutrients of continental origin. Although the Nile's impact on the pelagic environment has been much reduced by the construction of the Aswan High Dam, a significant concentration of water constituents still characterize the near-coastal zone in front of the delta, as seen in Plate 13. Turbulent diffusion from this area, and from the coastal zone downstream from the delta, with respect to the prevailing cyclonic circulation of the Levantine Basin, can be seen to shape the *chl* field, with various plumes extending offshore. Such a mechanism for biological enrichment of the eastern Mediterranean, supplying nutrients of coastal origin to the primary producers that sustain the food web in this otherwise oligotrophic region – nutrients that originate from the ever increasing use of fertilizers for agriculture, as well as from the proliferation of untreated sewage outfalls, due to population growth along the coast – has been suggested as the reason for the recent recovery of local fisheries, which had collapsed in the mid 1960's after the Nile damming (Nixon, 2004).

The Egyptian-Israeli-Lebanese coastal area appears as one of the main blooming “hotspots” in the preceding analysis of *chl* monthly anomalies. Hence, an attempt has been made to follow the development of coastal features in the south-eastern basin, through a series of SeaWiFS, MODIS and AVHRR images. The analysis concentrated in the spring-summer period, of 2001 and 2002 in particular, when the coastal dynamical processes of interest appeared to be most pronounced. Further, an attempt was also made to track the coastal features' origin using a spectral approach originally introduced by Karabashev *et al.* (2002), as well as a comparison between *chl* and sea surface temperature (*sst*) profiles.

#### **3.1 Spectral Signature of *chl* Patterns**

Based on spectral and chromaticity analyses (Bukata *et al.*, 1995), downstream waters along the coast show a decrease in suspended materials, dissolved organic matter and *chl*, possibly marking the northern limit of the Nile influence. A number of filaments and plumes are seen to extend close to populous cities and to recur rather systematically off Alexandria, the Gaza strip, Tel Aviv, Haifa, Tyre and occasionally Sidon, or at the mouth of *quasi*-perennial streams.

In order to determine the sources of the features anchored to the coast, series of “virtual stations” were determined for all major high-

*chl* plumes. Subsequently,  $L_{WN}$  spectra<sup>2</sup> were extracted from the images at successive stations along the coastal features. As noted above, the mixing between coastal and open sea waters has been highlighted following Karabashev *et al.* (2002). The spectra also give information on water composition in terms of Bukata *et al.*'s (1995) optical mixture model (pure water, chlorophyll and yellow substance).

Examples of the series of stations determined for the main filaments and plumes of the Egyptian-Israeli-Lebanese coastal area are given in Plate 14, where the SeaWiFS image collected on 4 June 2001 is displayed as a false-color composite of  $L_{WN}$  at 510, 490 and 443 nm. Optically well-defined features are marked off Alexandria, Gaza, Tel Aviv and Haifa, appearing as straight, meandering or spiralling patterns, up to 150 km long. Series of points have been superimposed on the main features of this image, to indicate the stations where spectra were extracted. Typical spectra obtained at these sites are shown in Plate 15, and can be summarized as follows:

- ü **Alexandria jet** (Plate 15, panel 1): the stations closer to the coast (1-6) show low  $L_{WN}$  in the blue channels and high  $L_{WN}$  in the green channels. Offshore,  $L_{WN}$  values gradually decrease first in channel 5, then in 4 and finally in 3, paralleled by an increase in channels 2 and 1. Station 12 has the typical spectral signature of blue oligotrophic water. In the plume, *chl* decreases from inshore ( $1.3 \text{ mg m}^{-3}$ ) to offshore waters ( $0.1 \text{ mg m}^{-3}$ ).
- ü **Gaza deflected plume** (Plate 15, panel 2): station 1 has water spectrally similar to that of Alexandria's station 1 (green waters, with high *chl*). The trend along the curved path of the plume is towards bluer waters, in spite of station 13 being close to the coast. This points to a distinct character of the plume itself, in which little mixing takes place with surrounding waters.
- ü **Tel Aviv straight filament** (Plate 15, panel 3): compared to those of Gaza and Alexandria, the Tel Aviv coastal waters are not as green, and *chl* is low ( $< 0.5 \text{ mg m}^{-3}$ ). Along the plume, the spectra evolve regularly towards the shape typical of blue waters.
- ü **Haifa deflected plume** (Plate 15, panel 4): the plume spectra are quite similar to those of the Tel Aviv straight filament.

### 3.2 Comparing *chl* and *sst* Patterns

In those cases when corresponding *chl* and *sst* data could be obtained, the filaments and plumes appearing at the same locations in each of the two images were compared. In general, both types of features, *i.e.*

---

<sup>2</sup> The spectra include  $L_{WN}$  for the 8 visible and near-infrared SeaWiFS channels, at 412 (1 violet), 443 (2 blue), 490 (3 blue-green), 510 (4 green), 555 (5 green-yellow), 670 (6 red), 765 (7 NIR1) and 865 (8 NIR2) nm; *chl* constitutes *pseudo*-channel 9.

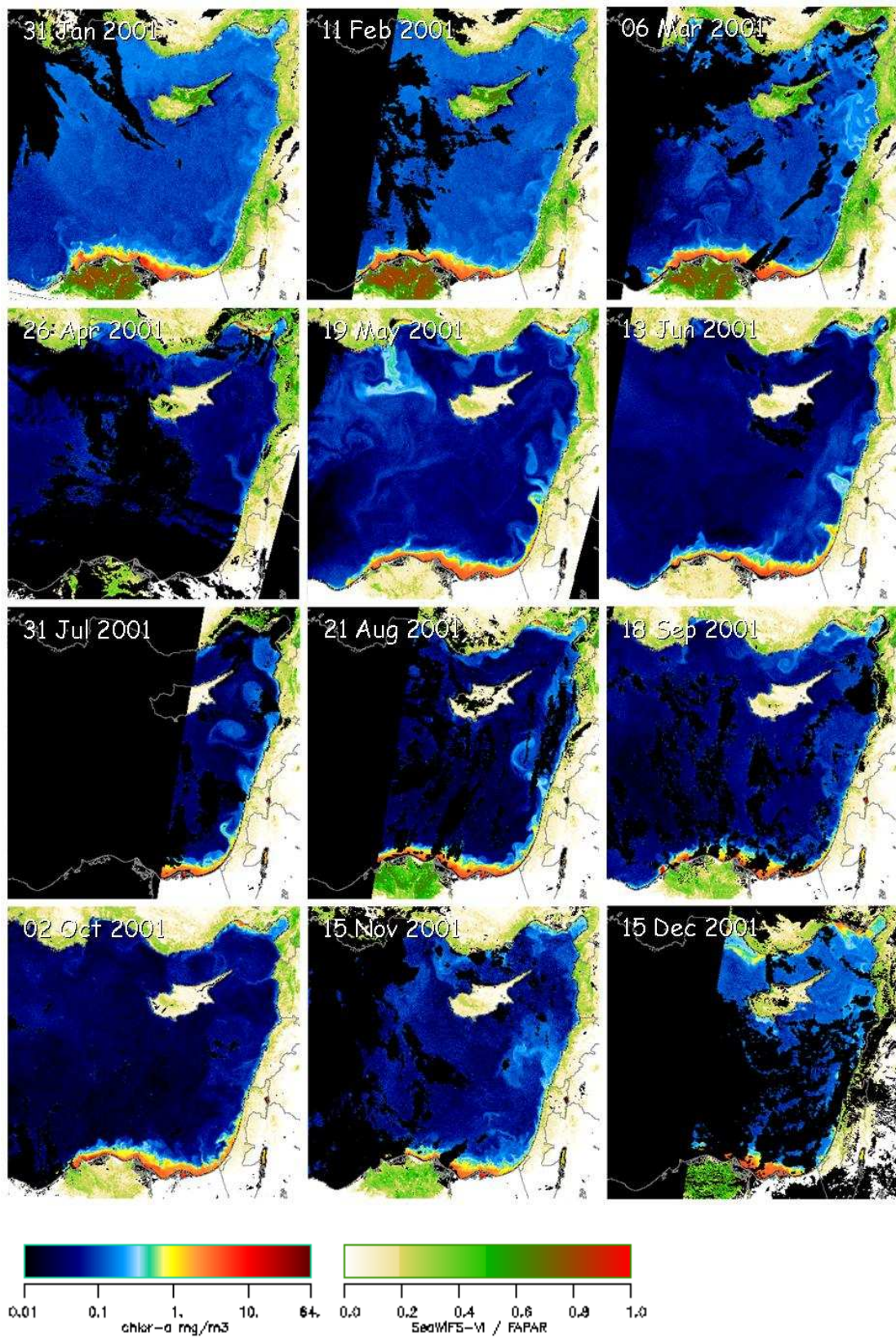
those traced by color and by temperature, showed a certain similarity in their shape, with greener waters corresponding to warmer waters. Plate 16 shows, as an example, *chl* and *sst* profiles extracted in the east-west and north-south directions across a coastal plume appearing in the MODIS image dated 1 August 2002 (the image is displayed in Plate 14 (bis), as a false-color composite of  $L_{WN}$  at 510, 490 and 443 nm, together with the series of stations where the profiles were extracted).

The temporal evolution of corresponding color and thermal patterns is shown in Plate 17. In the images dated 1 August 2002, the complex, two-lobe *chl* plume is rooted at the coast in the vicinity of Haifa. Five days later, in the images dated 6 August 2002, the same feature seems to have detached from the coast, and to drift northwards in a clockwise direction. This movement is amplified after five more days, in the images dated 11 August 2002, when the two lobes appear to be disjointed, the upper one being entrained southwards.

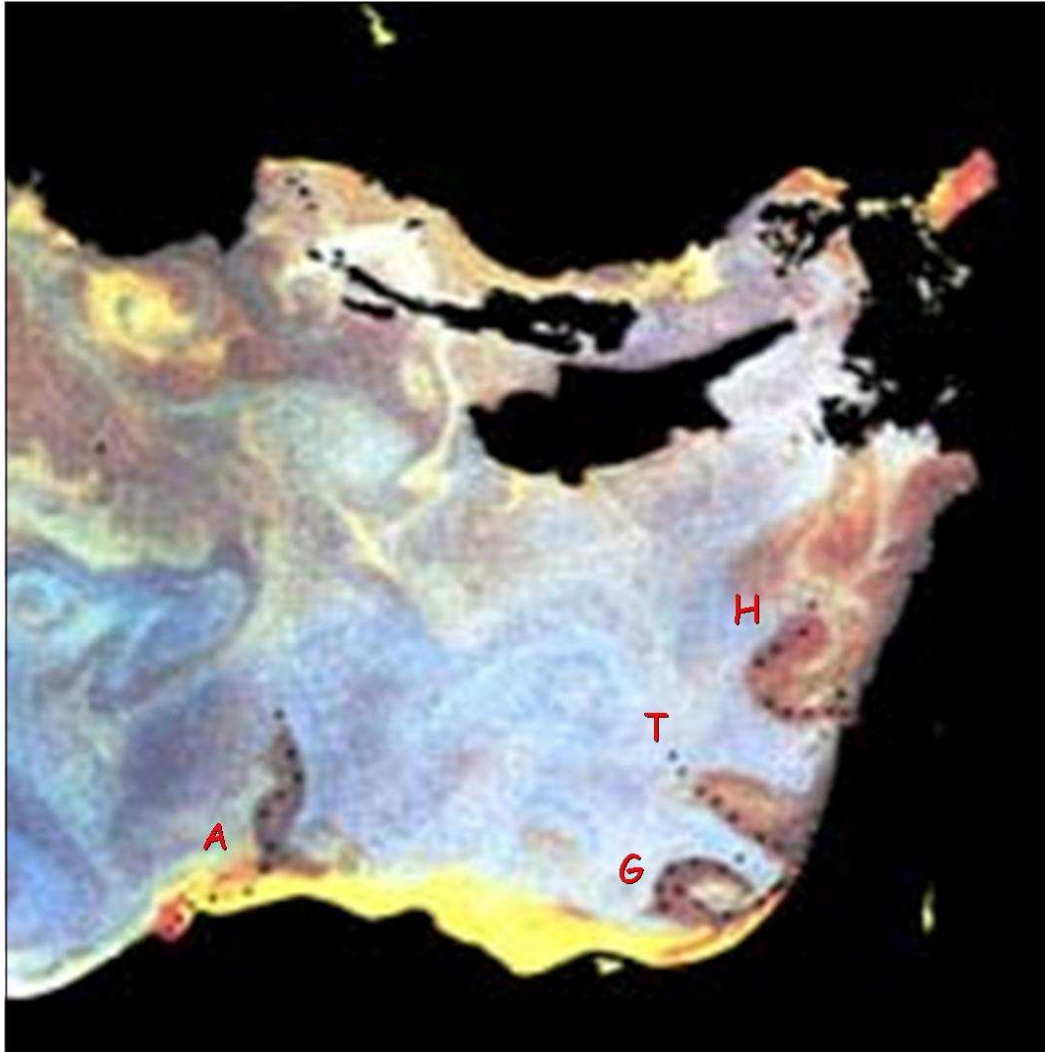
It is reasonable to assume that the enhanced *chl* values of the color plumes must be due to an additional supply of nutrients, with respect to local background concentrations. Then, the coincidence of higher-*chl* and higher-*sst* features would preclude the plumes from being due to a nutrient input by coastal upwelling of deep waters (which would imply lower *sst* values). Instead, the greener-warmer correspondence points towards a nutrient input from land-based sources. The major source would be the Nile delta river, sewer and agricultural runoff system, propagated northwards to some extent by the prevailing current (Alhammoud *et al.*, 2005), with additional sources from large coastal cities and from *quasi*-perennial streams. The large extent and long persistence of these features can be explained by the strong buoyancy of the warm, fresh water provided by the river and sewer inputs. These would be distributed offshore, from the margin of the northward current, by eddies influenced by the irregular topography of the continental shelf.



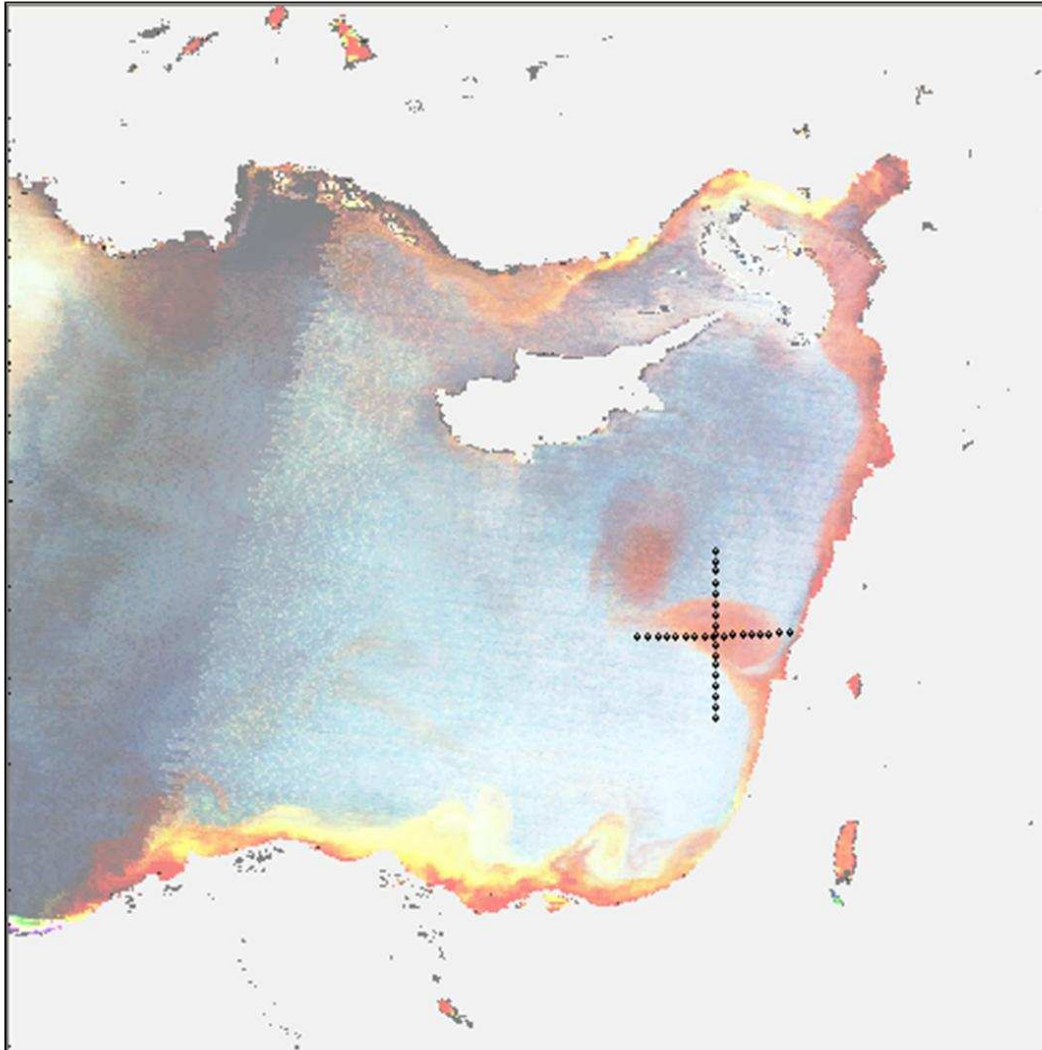
Plate 13. SeaWiFS-derived chl, SE Basin, 2001 Daily Images





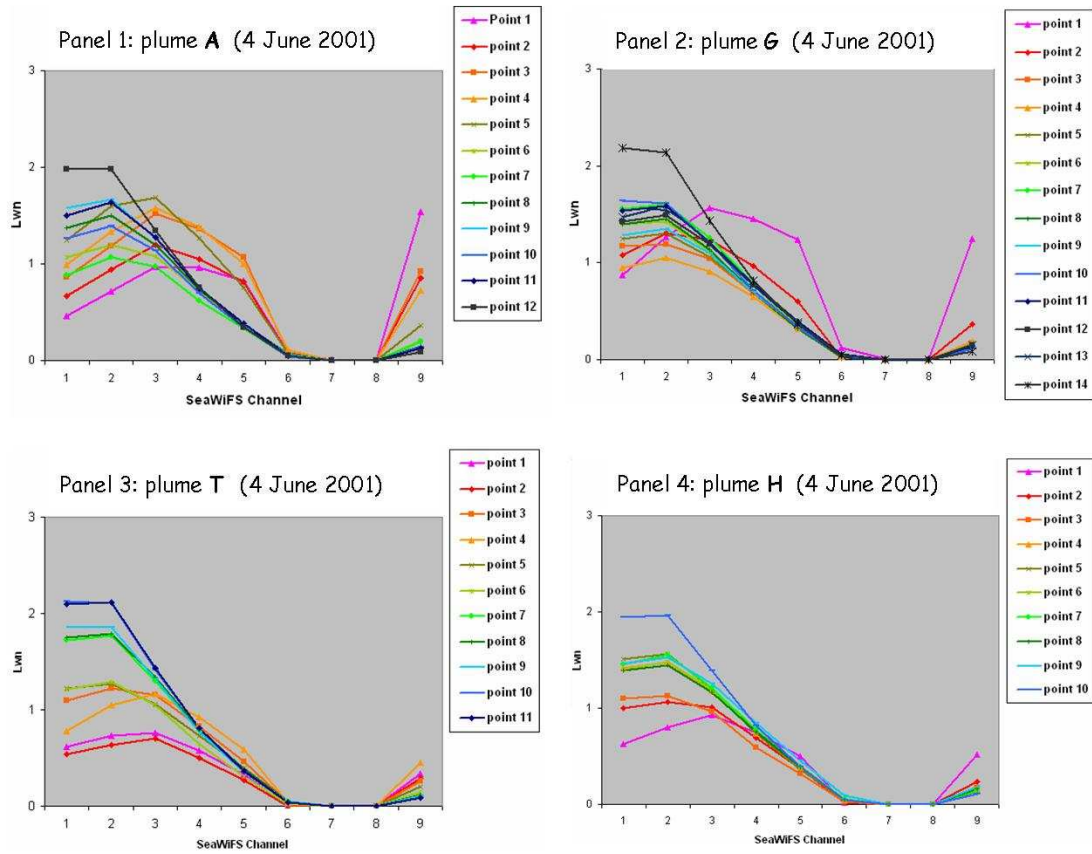


SeaWiFS -derived  $L_{WN}$  (4 June 2001). False-colour display of 3 channels (510, 490, 443 nm) with histogram equalization. The black dots indicate stations where spectra were computed for the Alexandria (A), Gaza (G), Tel Aviv (T) and Haifa (H) plumes.



MODIS -derived  $L_{WN}$  (1 August 2002). False-colour display of 3 channels (510, 490, 443 nm) with histogram equalization. The black dots indicate stations where profiles were extracted along the East-West and North-South directions within the Haifa plume.

Plate 15. SeaWiFS-derived  $L_{WN}$  Spectra in Coastal Plumes



$L_{WN}$  spectra along coastal plumes for the 8 SeaWiFS channels (4 June 2001).  
 Station numbers increase from the coast in the offshore direction.  
 Pseudo-channel 9 is chl in [ $mg\ m^{-3}$ ].

Plate 16. Profiles (EW and NS) of MODIS-derived chl and sst

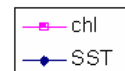
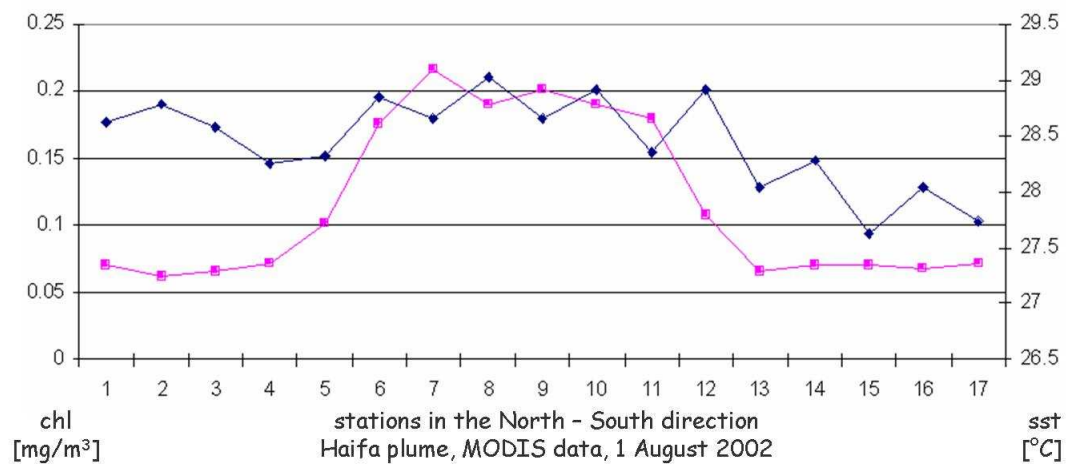
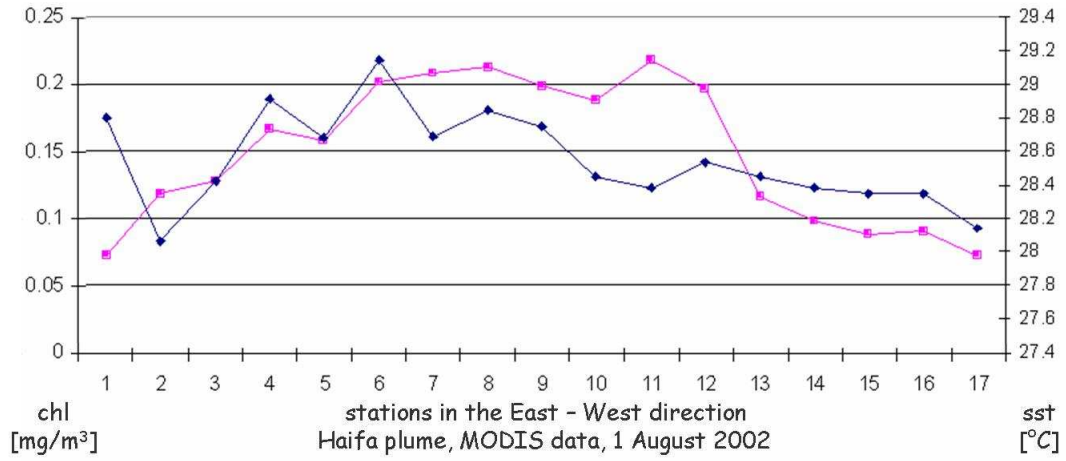
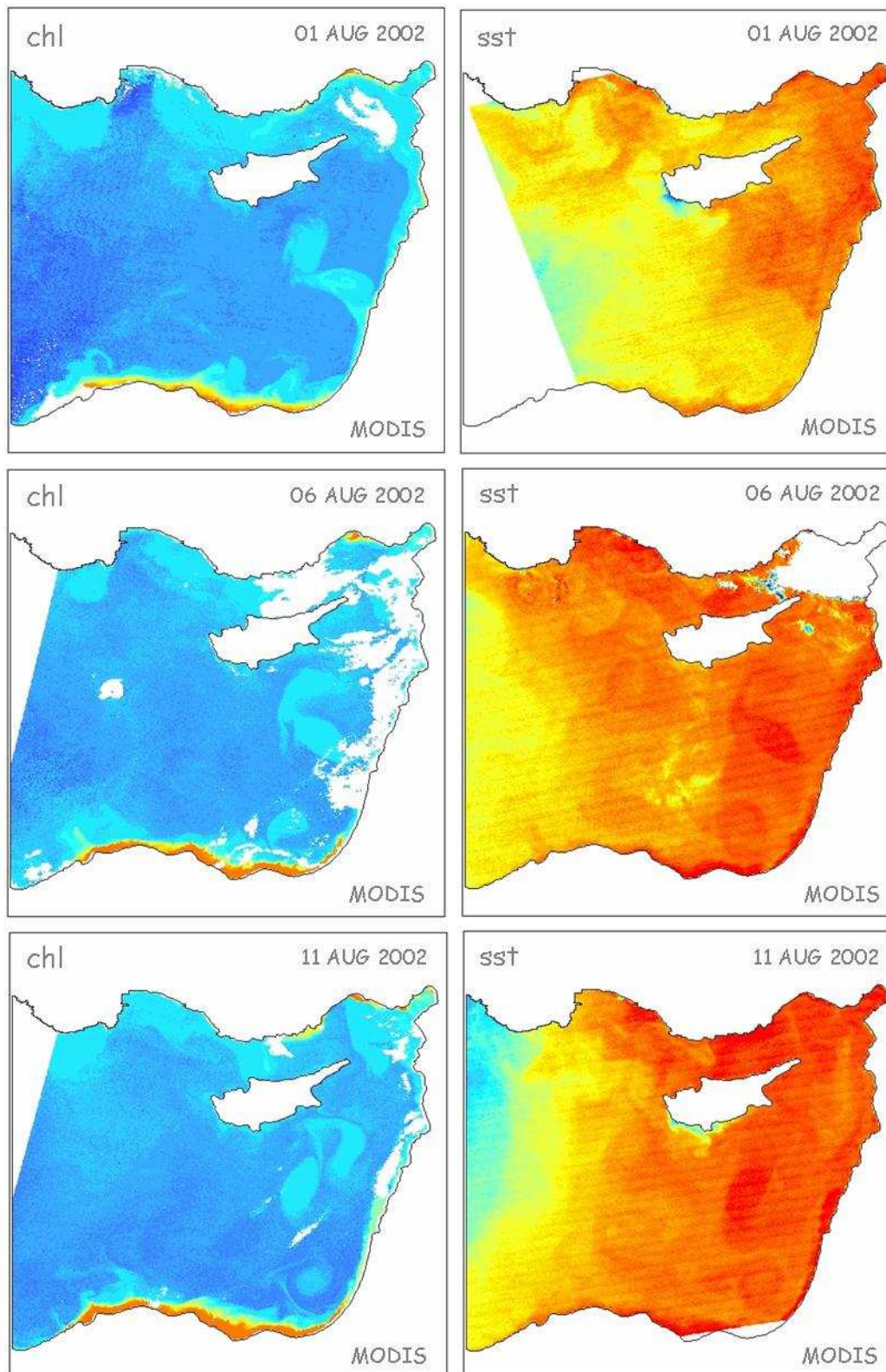




Plate 17. MODIS-derived chl and sst Patterns



The rainbow color table shows low chl / sst in blue and increasing values in green, yellow and red.



#### **4. Algal blooms in the western basin**

The SeaWiFS data set was used to explore the phytoplankton field of the near-coastal mesotrophic region in the western basin of the Mediterranean Sea, in connection with blooming episodes of *Alexandrium*, the dinoflagellate *genus* which causes most HABs in the basin. Various species of *Alexandrium* (*A. minutum*, *A. catenella*, *A. taylori*) have been recorded in the western basin, where blooming takes place primarily in near-coastal areas (a summary of recent episodes is reported in Plate 18). In particular, blooms have been recurring in the 1990s and 2000s at several sites along the Catalan coast, as well as at selected sites on the coast of Sardinia and of Sicily (see Annex 2). Interestingly, the emergence and recurrence of such *Alexandrium* blooms in the Mediterranean Sea seems to correspond to a general decreasing trend of the *chl* indicator, estimated to be on the order of 10% of the annual mean value for the entire basin, in the period of SeaWiFS coverage (Barale *et al.*, 2004).

Although a significant body of information exists on recurring *Alexandrium* blooms at local scales, in some cases it is difficult to demonstrate whether such blooms start in confined waters, or stem from episodes occurring in open waters, just on the basis of *in situ* studies (Vila *et al.*, 2001). Furthermore, if a bloom starts in confined waters, it is not clear whether, and under what circumstances, it can then be exported to open waters. The question arises to determine if there is any (qualitative) relationship between inshore HABs - of some target species, such as those of the *Alexandrium* genus - and large-scale, long-term offshore phytoplankton blooms, observed in satellite imagery. Hence, SeaWiFS images were used to trace phytoplankton dynamics at the regional scale for a multi-annual period (1998-2003). A qualitative comparison of these satellite data and *in situ* data from the Catalonia (as well as Sardinia and Sicily) shorelines was conducted for the last two years of the available period (2002-2003), when extensive data on *Alexandrium* blooming were collected at the coastal sites of interest (Annex 2; see Catalonia map in Plate A2).

##### **4.1 Comparing *in situ* and Satellite Data Records**

Examples of the decoupling between inshore and offshore regimes, even in those cases when they seem to co-vary, are provided by the monthly mean images of the north-western Mediterranean basin, for February, March and April 2002 and 2003 (Plate 19). In both years, a massive spring bloom is seen to develop off the Gulf of Lions, where the deep convection processes occurring in winter (note the patch of blue waters, the so-called "blue hole", in the February images) generate favorable conditions for blooming to occur (Barale, 2003). When the offshore structures develop, they appear to be more or less separated from the inshore ones by a tongue of blue waters, extending from the Ligurian-Provençal basin into the Balearic basin, possibly

corresponding to the southward-flowing Northern Current - *i.e.* the former Ligurian, Liguro-Provençal and Catalan Currents system (Millot, 1992). Only the March 2003 image suggests an exception to such conditions along the Catalan coastline. However, even in this case, the series of daily images composing the monthly mean (see below) demonstrate that the apparent continuity is actually due to a number of coastal plumes meandering in the offshore direction, which are merged together by the monthly compositing procedure.

The variety of surface features appearing along the Catalan coast, in the daily images for 2002 and 2003, can be observed in the series of Plate 20 and Plate 21. These comprise a selection of daily images chosen to represent the 12 months of both years. The *chl* values of the coastal patterns, color-coded to indicate the computed concentrations, can be compared with the total chlorophyll-a measured at various stations along the same stretch of shoreline (see Annex 2, Plate A3). Although some of the high *chl* events seen in the imagery do correspond, repeatedly in some cases, with the *in situ* chlorophyll-a relative maxima (*e.g.* in Arenys de Mar, between Barcelona and Tarragona, in Tarragona itself), in both years the general trend of the two data records does not present any consistent agreement. To the contrary, while the imagery appears to indicate a systematic *chl* maximum in late winter and early spring, followed by *chl* minimum in summer, the field data are characterized by summer maxima at most coastal stations. A comparison with the *Alexandrium* blooming record (see Annex 2, Plate A4) points to the fact that correspondences occur only episodically (*e.g.* L'Estartit, in May 2002, or Tarragona, in August 2003), while at other times opposite indications seem to come from the satellite and *in situ* data (*e.g.* Arenys de Mar, in February 2002, or between Barcelona and Tarragona, in June 2003).

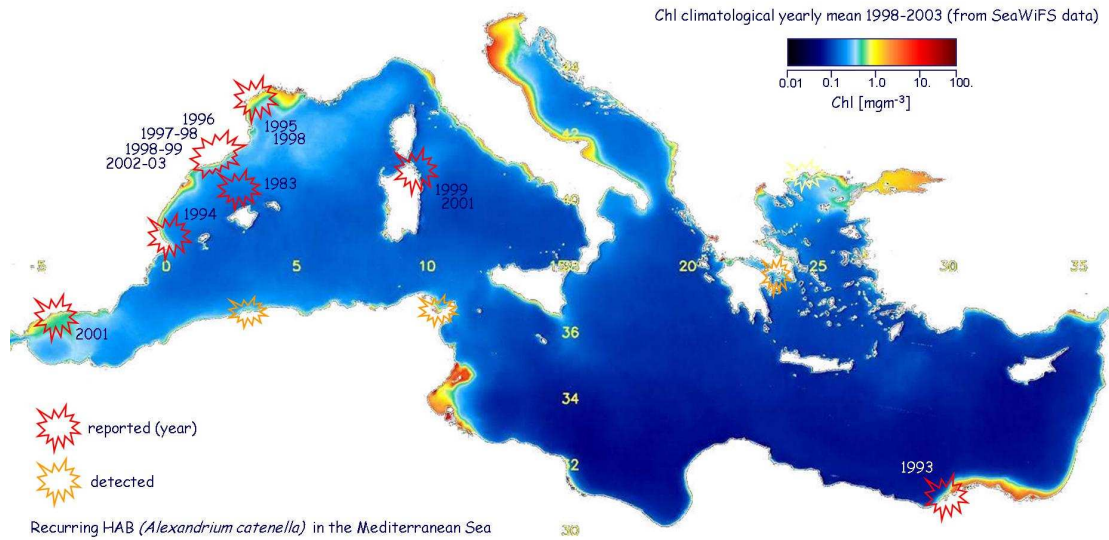
When considering interannual variability of the general blooming patterns, a striking coherence emerges from the satellite and *in situ* data records, as suggested by the images and stations of Sardinia. Plate 22 shows the monthly mean images for March 2002 and 2003, as well as some representative daily images selected among those used to compute the means. In both monthly mean images, higher *chl* values can be found east of the Strait of Bonifacio. This is possibly related to the vertical mixing and consequent enrichment of surface water with nutrients from deeper layers, induced by the funnelling effect of the Corsica and Sardinia orography on north-westerly winds and due to the ensuing dipole eddies created in the western Tyrrhenian basin. In the 2002 mean image, this feature is separated from the near-coastal regime of lower *chl* values, extending along the eastern coast of Sardinia, while the western coast presents somewhat higher *chl* values. Conversely, in the 2003 mean image, the same feature is connected to a pattern of convoluted structures, traced by higher *chl* values, extending southward along the eastern coast of Sardinia, while the western coast presents much lower values.



The total chlorophyll-*a* measurements (see Annex 2, Plate A5), performed in the same two months at Oristano, on the west coast, Porto Torres on the north coast and Olbia, on the east coast, offshore and inshore (3 km from the coastline and inside the corresponding harbors), show corresponding gradients in good agreement both for trends and absolute values. On the other hand, the remote sensor did not record the *maxima* occasionally reached by *Alexandrium* species in the Gulf of Olbia, in May/June 2002 and in April/May 2003 – which were associated to Paralytic Shellfish Poisoning (PSP) toxicity in mussels– possibly because these never reached typical “blooms” densities (*i.e.*  $>50 \times 10^3$  cells  $l^{-1}$ ).

Finally, the 2003 series of daily images, selected as the most representative for Sicily (Plate 23), shows a general agreement between satellite and *in situ* observations, at least in terms of general blooming areas and *in situ* hot spots with high *chl*. This is the case of the eastern (Ionian) coastline, where the highest *chl* values indicated by the imagery appear to be located in the Syracuse area and neighboring waters, consistently with the chlorophyll-*a maxima* of the *in situ* measurements (not shown here). In this area, a good correspondence can be observed in the spring record of the innermost coastal sites, as demonstrated by the *chl maximum* reached in April and the March/April bloom of *A. minutum* detected *in situ* (Vila *et al.*, 2005). In contrast, with the exception of some small features appearing in late winter, no significant high *chl* events were evidenced by the satellite along the northern (Tyrrhenian) coastline and the Aeolian Islands area, where localized events of water discoloration due to *A. taylori* outbreaks were monitored in summer, as in previous years, on Vulcano Island (Giacobbe *et al.*, 2005).

Plate 18. Recurring HABs (*Alexandrium catenella*), Mediterranean Sea



- 1983 open waters, NW Balearic front (Margalef & Estrada, 1987)
- 1994 confined waters, Valencia harbour (Gomis *et al.*, 1996)
- 1995-98 Thau lagoon, identified as *A. tamarense* (Lilly *et al.*, 2002)
- 1996 confined waters, Barcelona harbour (Vila *et al.*, 2001)
- 1997-98 confined waters, several harbours along southern Catalan coast (Vila *et al.*, 2001)
- 1998-99 open coastal waters off Catalonia, widespread blooms (Vila *et al.*, 2001)
- 1998 confined waters, Alexandria harbour (Mikhail, 2002)
- 1999-01 Gulf of Olbia (Luglié *et al.*, 2003), followed by first PSP event in 2001
- 2001 open coastal waters, monitoring station off Malaga (Fernandez *et al.*, 2004)
- 2002-03 confined waters, Tarragona harbour (STRATEGY, 2004)
- ... detections in Alger harbour (H. Illoul, p.c.), Bay of Tunis (S. Turki, p.c.), coastal sites in Greece (STRATEGY, 2004) ...

Plate 19. SeaWiFS-derived chl Monthly Means in the NW Basin

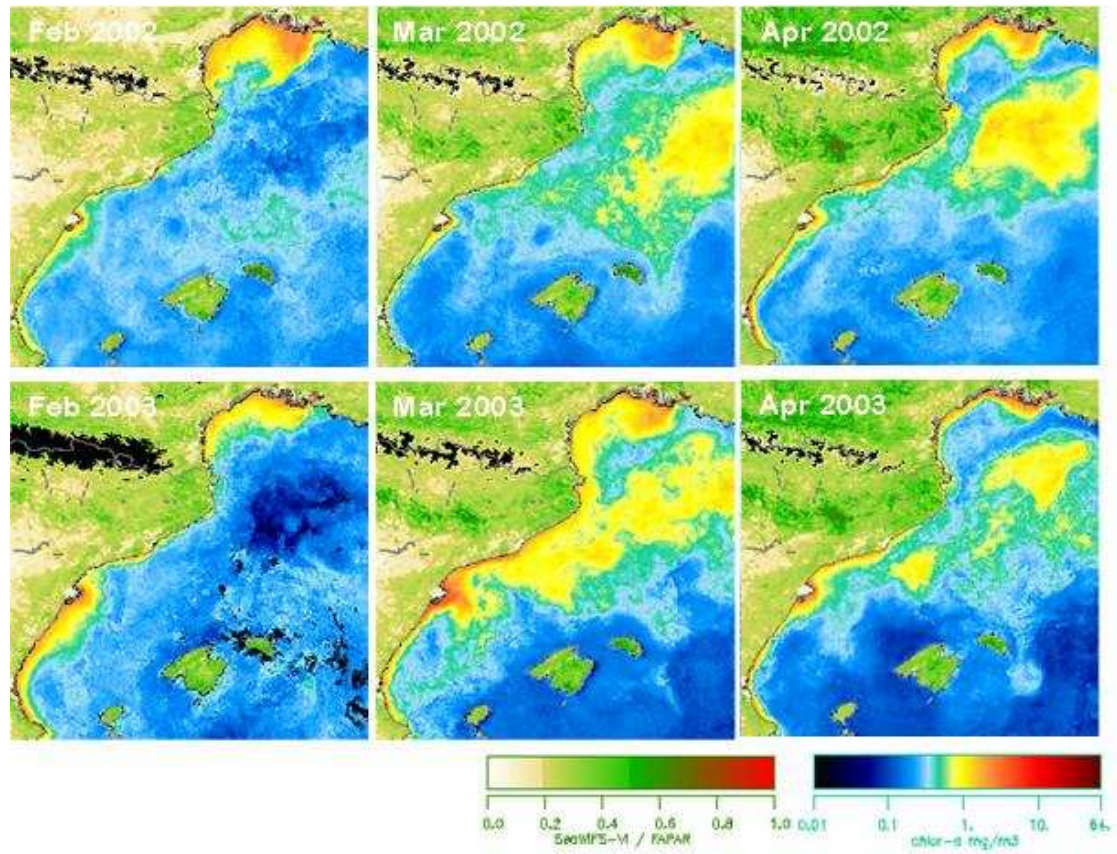




Plate 20. SeaWiFS-derived chl (Catalonia), 2002 Daily Images

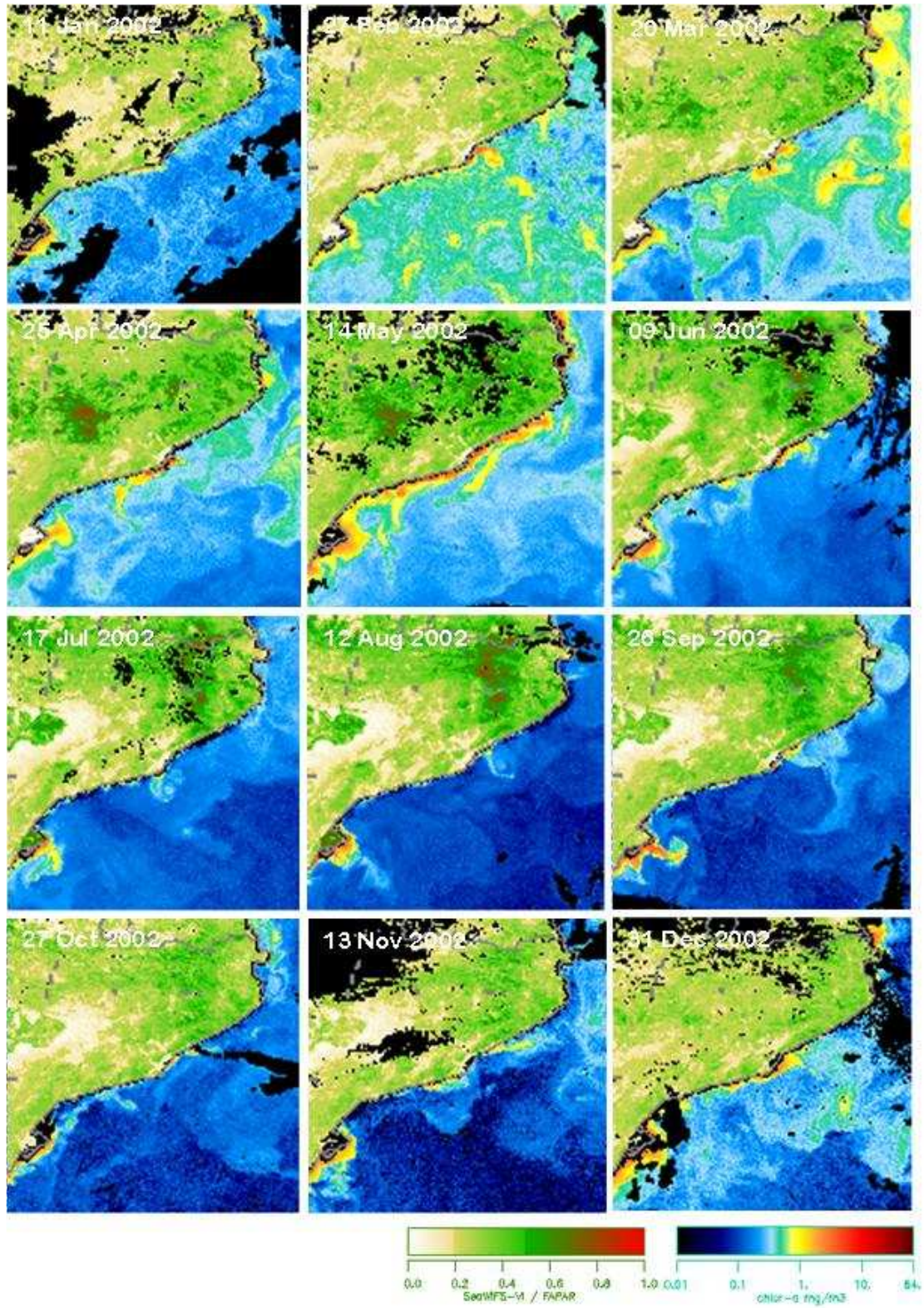




Plate 21. SeaWiFS-derived chl (Catalonia), 2003 Daily Images

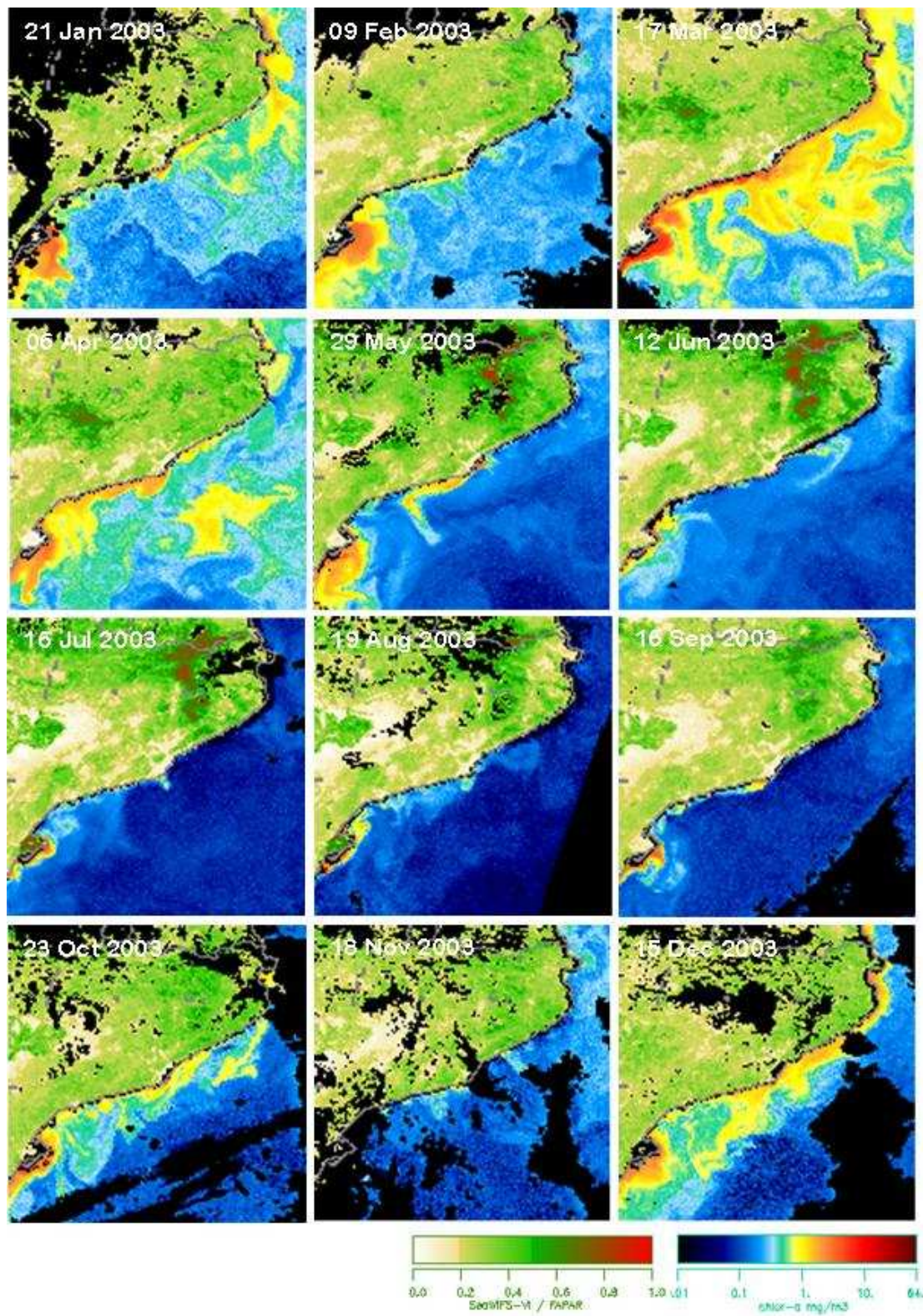




Plate 22. SeaWiFS-derived chl (Sardinia), March 2002/2003

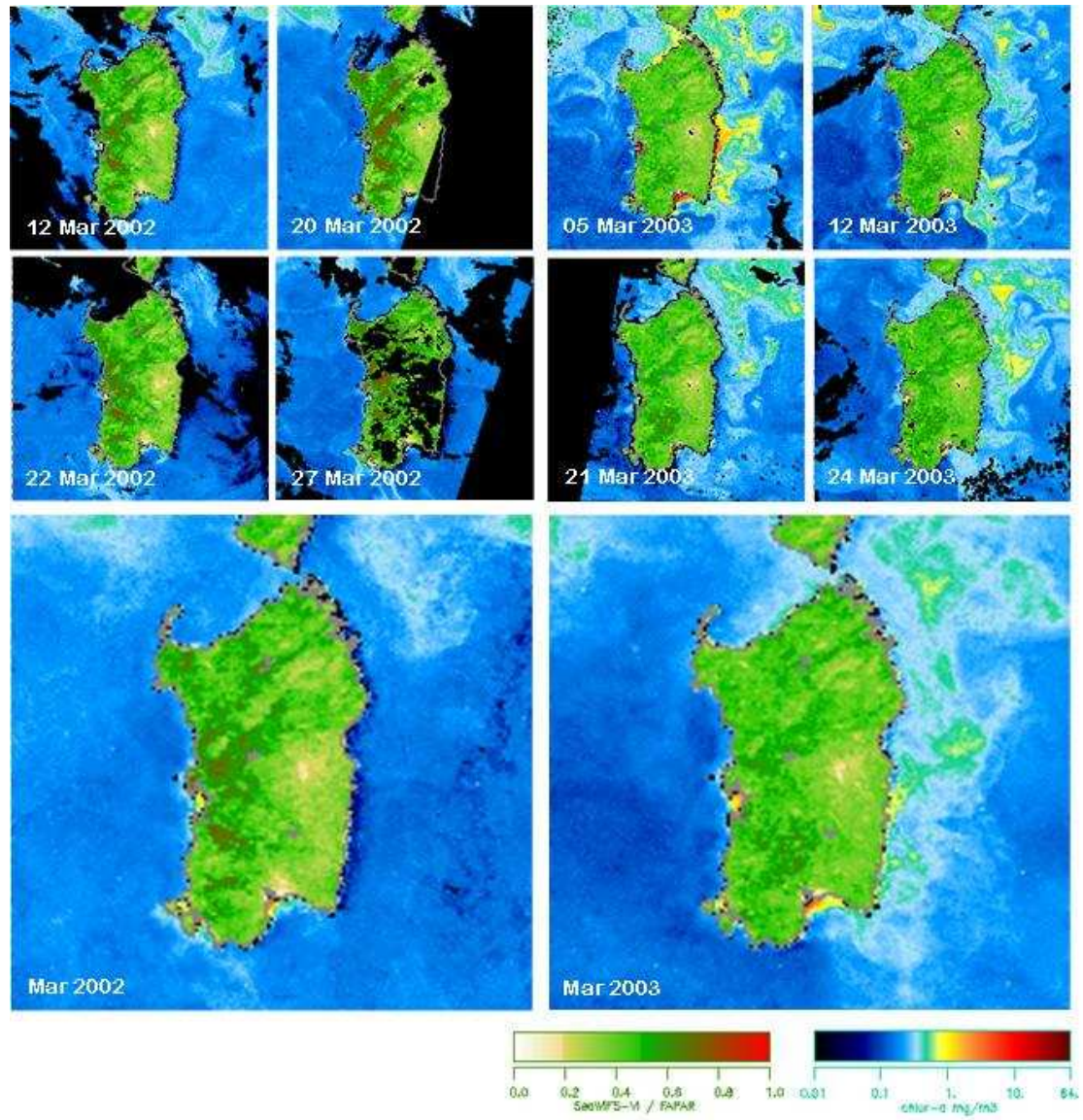
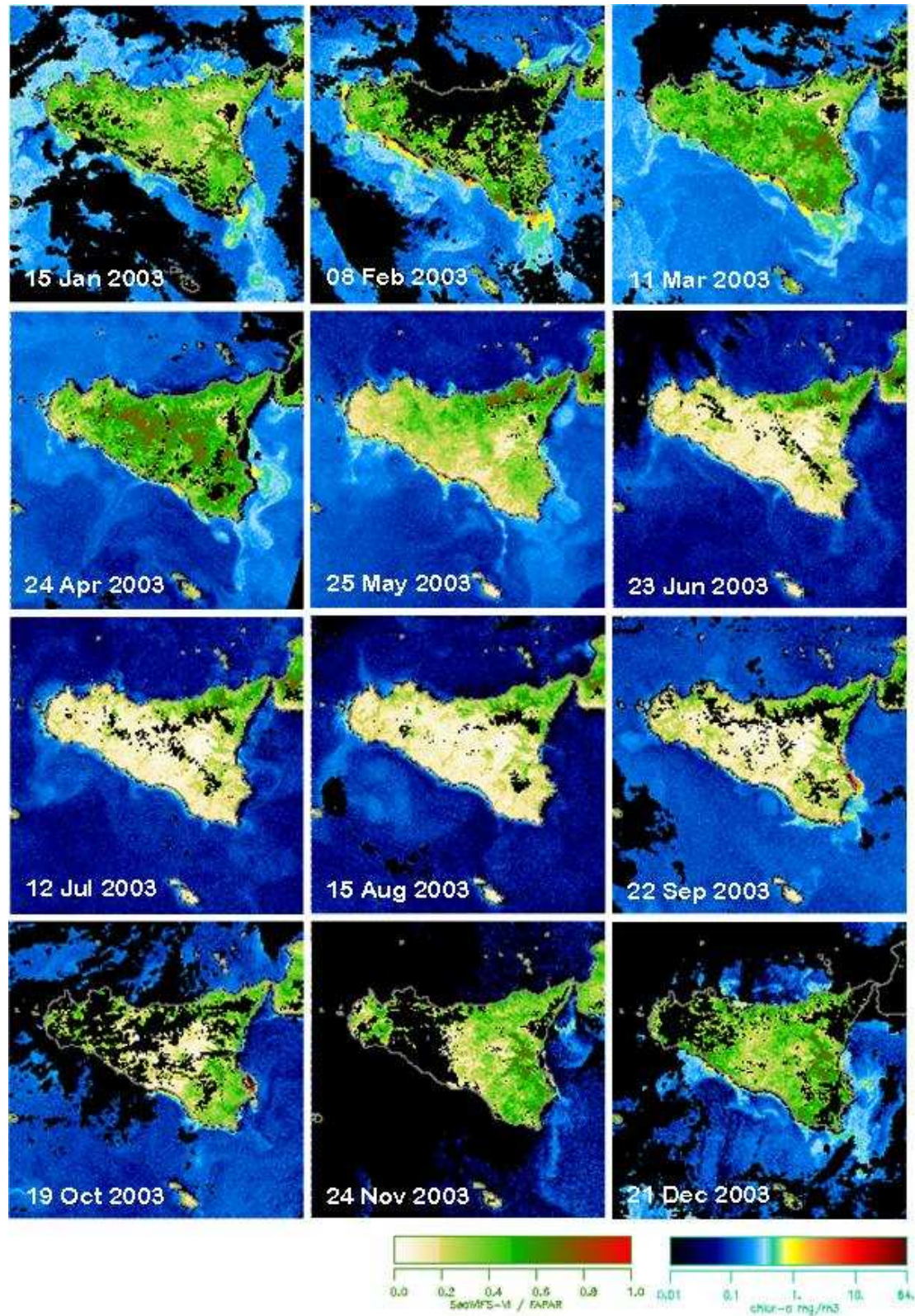




Plate 23. SeaWiFS-derived chl (Sicily), 2003 Daily Images







## 5. Conclusion and Future Activities

The analysis of SeaWiFS-derived *chl* maps has pointed out the kind of blooming anomalies that can occur in the Mediterranean Sea, as well as the hotspots where they seem to recur. Although the general trend between 1998 and 2003 appears to be one of decreasing anomalies, in line with a decrease of the *chl* average basin value (Barale *et al.*, 2004), some areas seem to follow an opposite tendency. Most notably, coastal areas in the south-eastern and in the north-western parts of the basin display intense local blooms shaped as filaments and eddies.

The south-eastern coastal area – *i.e.* the Egyptian-Israeli-Lebanese coast – is oriented in the SW-NE direction (see Plate 5, panel 3). The dominant current flows northward (Millot and Taupier-Letage, 2005), redistributing along its path a large input of suspended and dissolved matter, likely to include a sizeable nutrient load, from the Nile river. The coastal plumes, predominantly perpendicular to the shoreline, occur throughout the year, but are better seen in summer, when they contrast strongly with the ultra-oligotrophic character of the Levantine basin. Although the plumes are highly dynamical and change their shape frequently, the location of their “roots” on the coast is rather stable, corresponding to sites of major (urban) runoff.

The north-western coastal area – *i.e.* the Catalan coast – is oriented in the NE-SW direction (see Plate 5, panel 2), with a predominant current flowing southward (Millot and Taupier-Letage, 2005). Two main potential sources of suspended and dissolved matter, likely to provide a large amount of nutrients too, are present along this coast: the greater Barcelona area, corresponding also to the Llobregat river mouth, and the Ebro river delta. The Ebro plume is *quasi* permanent, but extremely variable in size (1 to 100 km), with *maxima* in winter-spring, presumably for hydrological reasons. The Barcelona plume is smaller (1-10 km, even absent at times), and is often connected to other minor features, which correspond to a number of small urban areas along both the northern and the southern stretches of coast.

These two coastal area present a number of similarities, which can be traced back to the presence of (i) (presumed) large nutrient sources of continental origin; (ii) patterns traced by high water constituents concentrations, rooted at specific coastal sites; (iii) strong current systems, inducing an alongshore drift of the coastal plumes, as well as their offshore spreading by turbulent processes. The main difference is that, although many point sources of runoff are scattered at (urban) sites along the coast, the main supply is located upstream in the Levantine case (the Nile), whereas it is downstream in the Catalan case (the Ebro). Further, the high-*chl* features off the Levantine coast are larger, and better recognizable against an oligotrophic background, while those off the Catalan coast have smaller size, and

tend to merge with co-varying larger patterns, when extending offshore. In both cases, the *chl* anomalies show an increasing positive trend, in the 1998-2003 period, which tallies with a growing “biological dynamism” at these sites (i.e. the expansion of coastal fisheries, in the south-east, and the intensification of noxious or harmful blooms in the north-west).

The present analysis suggest that – whereas the filaments and plumes in the Levantine seem to interact with large mesoscale dynamical features, such as offshore eddies or current meanders, typical of that part of the basin – the blooms along the Catalan coast are confined to the near-coastal zone, and seldom connect with offshore patterns. Indeed, the recurrent blooms in the western basin have been described as localized phenomena (see various authors in Masó, 2004), linked to increased nutrient availability and/or low water renewal, owing to the anthropogenic impact at the coastal sites (*e.g.* crowded beaches or marinas) or to specific geographical and meteorological conditions (*e.g.* enclosed bays during summer, when hydrodynamic forcing is low).

This would suggest that noxious, or harmful, blooms – at least in the areas and periods considered – are local phenomena, with little or no connection to regional events. Indeed, the isolated blooms detected at coastal Catalan stations in late-winter and early-spring coincide only occasionally with the regional type of blooming seen in the imagery – except perhaps for the 2003 late-winter, early-spring bloom, which affected the whole north-western Mediterranean. Later on in the year, in offshore waters – where thermal stratification progresses and the surface layer becomes nutrient depleted, with possible development of a deep chlorophyll *maximum* – the large-scale, regional blooms seen in the satellite imagery fade away. To the contrary, the stabilization of inshore waters – where nutrient concentration may be quite constant, for the entire annual cycle, in fact – continues to favor the growth of smaller-scale dinoflagellate blooms (Masó, 2004). Thus, in summer, many coastal blooms can occur, in the surface layer, even though not necessarily at scales accessible to the RS tools used here.

The impression emerging from the present attempt to reconcile satellite and *in situ* assessments of algal blooms, due to the very nature of the measurements performed in each case, is that of comparing phenomena occurring at different space and time scales. The *in situ* data describe phenomena extending over much smaller scales, and developing in shorter times, than those seen in the satellite data, which provide measurements integrated over larger areas and longer periods. Consequently, there appears to be hardly any correlation between the blooming areas/periods seen in the satellite and the *in situ* data record.

This would be an interesting preliminary result: it would essentially mean that the processes - the forcing functions - shaping the local (harmful) algal blooms and the regional blooms are different, or overlap only marginally. What matters locally seems to hardly have any effect at scales even slightly bigger (hence environmental impact, environmental sampling networks to monitor that impact, as well as remedies to that impact, can and should be addressed at the local level). Furthermore, large-scale phenomena, which matter at the basin level, may have a widespread impact, but can be easily overwhelmed, locally, by much-smaller-scale processes.

The lack of correlation between satellite and *in situ* data would be due to the patchiness of the “local” measurements (say at scales between 1 and 100 m, in any case well below the 1000 m order of magnitude for the picture elements of satellite images), which is simply not seen from space. Further, since “regional” measurements also present a certain degree of patchiness (say at scales between 1 and 100 km, this time), it might be concluded, ultimately, that this is the result of different forcing functions, acting at different space/time scales. Thus, local measurements cannot be taken as representative of “larger scale” phenomena, while the satellite data might be useful to place local events into a regional context, but not to explore the dynamics of “smaller scale” phenomena, which require direct, *in situ* monitoring.

Future activities of the present research program will aim to a better understanding of the issues above, and will include additional work on both blooming anomalies and comparisons of satellite and *in situ* data. The application of a new anomaly algorithm, based on the difference between short-term (10-day) *chl* mean values and a background (monthly) running mean value, will allow an improved assessment of blooming dynamics in the known hotspots of the basin. A key factor to understand bloom origin and dynamics, at the observed hotspots, can be obtained from the relation between *chl* and *sst* patterns. This has been clearly established for the Levantine coast, pointing to a likely continental origin for the nutrients triggering the coastal blooms. Similar work should be carried out also for other near-coastal hotspots (*i.e.* the Catalan coast, primarily, but also the entire Gulf of Lions region, or the Adriatic basin), as well as for pelagic zones characterized by increasing positive *chl* anomalies (such as that south and east of Crete). Finally, a quantitative comparison with *in situ* measurements should be attempted, keeping in mind the well-known limitations of remote *chl* assessments, in order to explore the potential for assimilation of RS data into HAB monitoring and/or predicting schemes.

## References

- Alhammoud, B., K. Béranger, L. Mortier, M. Crépon & I. Dekeyser (2005). "Surface circulation of the Levantine Basin: Comparison of model results with observations". *Progress in Oceanography*, vol. 66, p. 299-320.
- Barale, V. (1994). "Ocean colour, planktonic pigments & productivity". *Memoires de l'Institut Oceanographique, Monaco*, n. 18, p. 23-33.
- Barale, V. (2003). "Environmental Remote Sensing of the Mediterranean Sea". *Journal of Environmental Science and Health*, vol. A38 (8), p. 1681-1688.
- Barale, V., B. Weber & J.M. Jaquet (2004). "*Bio-optical Environmental Assessments of Marginal Seas. Progress Report 1*". European Commission, EUR 21479 EN, pp. 50.
- Bukata, R.P., J.H. Jerome, K.Y. Kondratyev, D.V. Pozdnyakov (1995). *Optical Properties and Remote Sensing of Inland and Coastal Waters*. CRC Press, pp. 362.
- Fu, G., K.S. Baith & C.R. McClain (1998). "SeaDAS: The SeaWiFS Data Analysis System". In: *Proceedings of the 4th Pacific Ocean Remote Sensing Conference*, Qingdao (China), 28-31 July 1998; p. 73-7.
- Giacobbe, M.G., A. Penna, E. Gangemi, M. Masò, E. Garcès, S. Faga, I. Bravo, F. Azzaro, F. Dicembrini & N. Penna (2005). "Recurrent high-biomass blooms of *Alexandrium taylorii* (Dinophyceae), a HAB species expanding in the Mediterranean Sea". *Hydrobiologia* (in press).
- Hooker, S.B., W.E. Esaias, G.C. Feldman, W.W. Gregg & C.R. McClain (1992). "An Overview of SeaWiFS and Ocean Color", SeaWiFS Technical Report Series, Vol. 1, S.B. Hooker and E.R. Firestone ed.s, NASA Technical Memorandum 104566, pp. 25.
- Jaquet, J.M., S. Tassan, V. Barale & M. Sarbaji (1999). "Bathymetric and bottom effects on CZCS chlorophyll-like pigment estimation: data from the Kerkennah shelf (Tunisia)". *International Journal of Remote Sensing*, 20 (7), p. 1343-1362.
- Karabashev, G., M. Evdoshenko & S. Sheberstov (2002). "Penetration of coastal waters into the Eastern Mediterranean Sea using the SeaWiFS data". *Oceanologica Acta*, vol. 25, p. 31-38.
- Masó M, ed. (2004). "*Proceedings of the Workshop on Management of recreational waters in relationship with Harmful micro-Algae*

- Blooms (HAB) in the Mediterranean Sea*". Institut de Ciències del Mar, Barcelona, Spain, pp. 39.
- Melin, F., B. Bulgarelli, N. Gobron, B. Pinty & R. Tacchi (2000). "An integrated tool for SeaWiFS operational processing". European Commission Publication, no. EUR 19576 EN, Ispra (Italy).
- Millot, C. (1992). "Are there major differences between the largest Mediterranean seas? A preliminary investigation". *Bulletin de l'Institut Océanographique, Monaco*, vol. 11, p. 3-25.
- Millot, C. & I. Taupier-Letage (2005). "Circulation in the Mediterranean Sea". In: Handbook of Environmental Chemistry, Volume 5 Water Pollution, Part K, *The Mediterranean Sea*, A. Saliot ed., Springer, Berlin, Heidelberg, New York, p. 29-66.
- Moran, P.A.P. (1950). "Notes on continuous stochastic phenomena", *Biometrika*, vol. 37, p. 17-23.
- Nixon, S.W. (2004). "The Artificial Nile", *American Scientist*, vol. 92, p. 158-165.
- Sturm, B. and G. Zibordi (2002). "SeaWiFS atmospheric correction by an approximate model and vicarious calibration". *International Journal of Remote Sensing*, vol. 23 (3), p. 489-501.
- Vila, M., E. Garcés, M. Masó and J. Camp (2001). "Is the distribution of the toxic dinoflagellate *Alexandrium catenella* expanding along the North West Mediterranean coast? ". *Marine Ecology Progress Series*, vol. 222, p. 73-83.
- Vila, M., M.G. Giacobbe, M. Masó, E. Gangemi, A. Penna, N. Sampedro, F. Azzaro, J. Camp & L.A. Galluzzi (2005). "A comparative study on recurrent blooms of *Alexandrium minutum* in two Mediterranean harbors". *Harmful Algae*, vol. 4, p. 673-695.
- Weber, B., J.M. Jaquet & G. Faour (2004). "Cartographie et origine des panaches chlorophylliens côtiers en Méditerranée orientale à partir des images de SeaWiFS et d'ETM+ de Landsat 7". *Téledétection*, Special Issue, vol. 4 (2), p. 175-195.





## **Annex 1**

### *The Chlorophyll Auditor <sup>TM</sup> Software*

#### Components

The *Chlorophyll Auditor <sup>TM</sup>* software, coded in java<sup>TM</sup>, consists of the following elements:

- Files packet: it handles files, their loading and subsetting. It also takes care of memory allocation and determines the optimal strategy for the computations. It comprises four classes devoted to these various tasks.
- Process packet: it is in charge of computations, data masking and multi-threading. It also handles all the parameters controlling the processes (seven classes).
- View packet: it handles the display of the results as maps with legends, graphs and histograms (six classes).

In addition to these packets, two additional segments deal with the coordination of tasks during runtime and error/warning messages.

#### Interface

The software is accessible via the interface shown in Plate A1. The zones numbered and marked in red have the following functionalities:

(1) Command buttons, with:

- « Options » to select basic options such as mask choice,
- « Compute » to enter options, file paths/names, I/O functions,
- « Image » to load and display a result as an image,
- « Mask » ,
- « Stop » ;

(2) Selection combo for color palette;

(3) Tabs :

- « Console », unique, to display infos on the ongoing process,
- « Histogram », unique, to load a dataset and histogram display,
- « Image », multiple. It loads each image of each file separately;

(4) Progress bar indicator;

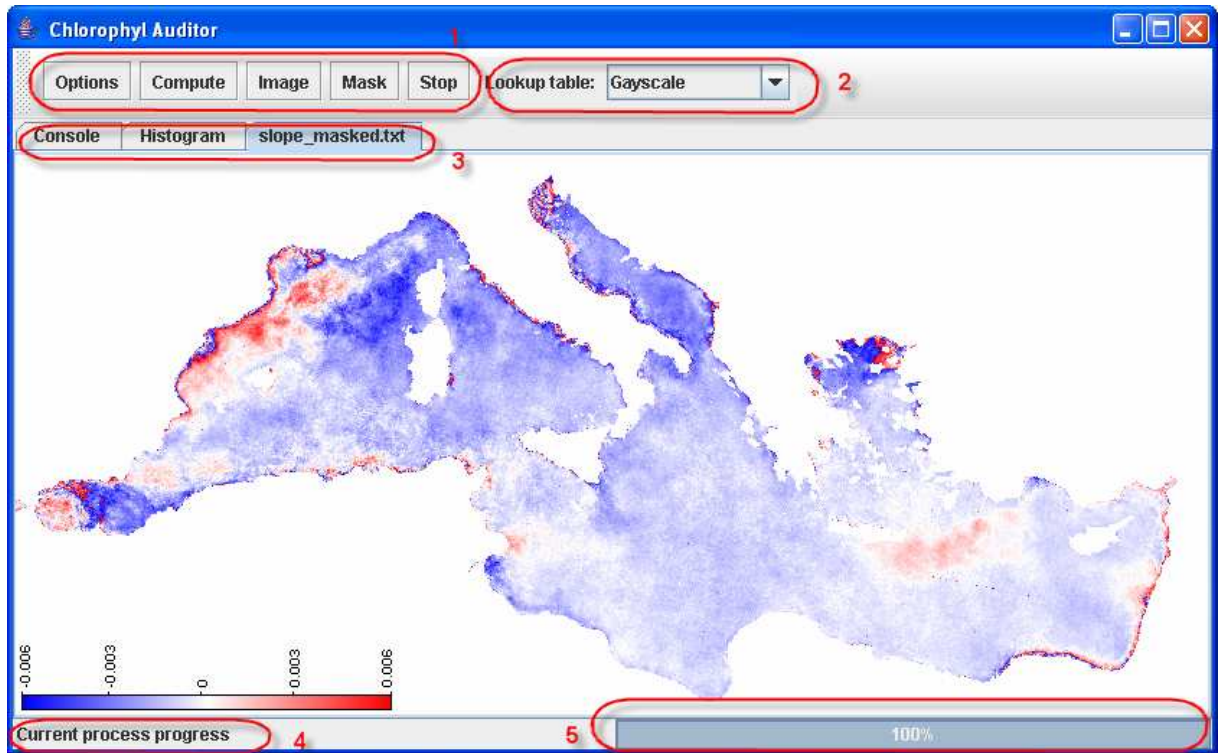
(5) Progress bar (0-100%).

The complete java<sup>TM</sup> code (30 pages) for all the component is given in Ndiaye (2006) and can also be obtained from the authors ([mapathe.ndiaye@terre.unige.ch](mailto:mapathe.ndiaye@terre.unige.ch)).

#### *Reference*

Ndiaye M., 2006. Etude statistique des anomalies de la concentration en chlorophylle en Méditerranée, sur la base des données SeaWiFS (1998-2003) et au moyen du logiciel Chlorophyll Auditor <sup>TM</sup>. Certificate of Geomatics, University of Geneva, p. 67.

Plate A1. Total chlorophyll-a, Sardinia coastal stations, March 02/03



## Annex 2

### *The Alexandrium genus in situ data record.*

Various species of *Alexandrium* have been recorded in the western Mediterranean basin, in the late 1990s and early 2000s. Blooms have been recurring primarily in near-coastal areas along the shorelines of Catalonia (Vila *et al.*, 2001; Vila and Masò, 2005), as well as at selected coastal sites of the Sardinia (Lugliè *et al.*, 2003) and Sicily (Penna *et al.*, 2002; Vila *et al.*, 2005). The bloom types range from those of noxious species (*e.g.* *A. taylori*), generating elevated biomasses and causing a deterioration of coastal water quality along popular beaches, to those of toxic species (*e.g.* *A. minutum* and *A. catenella*), exhibiting a rapid geographical spread during the past decade, mostly in harbors and shellfish farms, and causing repeated sanitary alarms and substantial economic losses.

A number of stations were examined in 2002-2003 – in the framework of the EC FP 5 STRATEGY Project (Masò, 2003) – along the coast of Catalonia, of Sardinia and of Sicily - to establish the distribution of 3 target *Alexandrium* species, *i.e.* *A. minutum* Halim, *A. catenella* (Whedon & Kofoid) Balech and *A. taylori* Balech, in each area. Given that blooms of *Alexandrium* in the Mediterranean Sea are observed in two main types of coastal environment, *i.e.* harbors/bays (*A. minutum*, *A. catenella*) and beach areas (*A. taylori*), the stations selected for sampling included both kinds of systems. In order to qualify the results reported here, it should be pointed out that the field sampling points were selected as representative of the potentially worse environmental situation, in the most confined areas, and not as representative of the general characteristics in a given area.

Temperature and salinity were measured *in situ* and water samples were collected at the surface for nutrients, phytoplankton and chlorophyll-*a* analyses. The samples were Lugol's fixed, settled and counted in an epifluorescence inverted microscope. Cells were stained with calcofluor and identified following Balech 1995. A detailed description of methods is given in papers enumerated above for the 3 areas studied. In Catalonia, sampling in harbors was carried out on 2 to 4 occasions per month, from March to September, and once or twice a month for the rest of the year. Catalan beaches were sampled once a week in summer. A similar sampling frequency was used to monitor coastal areas of Sardinia and Sicily.

A summary of the results obtained at the Catalan coastal stations (see map in Plate A2), in 2002 and 2003, for total chlorophyll-*a* and *Alexandrium* blooms are shown in Plate A3 and Plate A4, respectively. Further, total chlorophyll-*a*, measured at selected coastal stations of Sardinia, in March 2002 and 2003, is shown in Plate A5.

## Acknowledgements

Financial support for the field activities described in the present Annex was provided by the European Commission (EC) FP5 Project STRATEGY (EVK3-CT-2001-00046), by the Agència Catalana de l'Aigua (Department de Medi Ambient, Generalitat de Catalunya) and by CSIC through the contract "Pla de vigilància de fitoplàncton nociu a la costa Catalana". Thanks are due to Mercedes Masó and Magda Vila, Institut de Ciències del Mar, Barcelona (E), to Antonella Lugliè and Nicola Sechi, Università di Sassari, DBEV, Sassari (I), and to Maria Grazia Giacobbe, Istituto Ambiente Marino Costiero, CNR, Messina (I), for generously providing the in situ measurements shown here, in the framework of an informal co-operation agreement with the Institute for Environment and Sustainability, Joint Research Centre of the EC.

## References

- Vila, M., J. Camp, E. Garcés, M. Masó & M. Delgado (2001). High resolution spatio-temporal detection of potentially harmful dinoflagellates in confined waters of the NW Mediterranean. *Journal of Plankton Research*, vol. 23, p. 497-514.
- Vila, M. & M. Masó (2005). Phytoplankton functional groups and harmful species in anthropogenically impacted waters of the NW Mediterranean Sea. *Scientia Marina*, vol. 69, p. 31-45.
- Lugliè, A., MG. Giacobbe, F. Fiocca, A. Sannio & N. Sechi (2003). The geographical distribution of *Alexandrium catenella* is extending to Italy! First evidences from the Tyrrhenian Sea. In: *Harmful Algae 2002*, edited by A Steidinger, JH Landsberg, CR Tomas & GA Vargo (Florida Fish & Wildlife Conservation Commission & IOC UNESCO, St. Petersburg), p. 329-331.
- Penna, A., MG. Giacobbe, N. Penna, F. Andreoni & M. Magnani (2002). Seasonal blooms of the HAB dinoflagellate *Alexandrium taylori* Balech in a new Mediterranean area (Vulcano, Aeolian Islands). *P.S.Z.N. Marine Ecology*, vol. 23, p. 1-9.
- Vila, M., MG. Giacobbe M. Masó, E. Gangemi, A. Penna, N. Sampedro, F. Azzaro, J. Camp & L.A. Galluzzi (2005). A comparative study on recurrent blooms of *Alexandrium minutum* in two Mediterranean harbors. *Harmful Algae*, vol. 4, p. 673-695.
- Masó, M. & the STRATEGY Group (2003). New strategy of monitoring and management of HABs in the Mediterranean Sea (STRATEGY): an EU research program. In: *Proceedings of the 6th International Conference on the Mediterranean Coastal Environment, MEDCOAST 03*, E. Özhan ed., METU, Ankara (TR), vol. II, p. 931-940.

Plate A2. Catalan coast.



Map of Catalonia. Selected coastal station for total chlorophyll-a and *Alexandrium* blooms reported in text.

Plate A3. Total chlorophyll-a, Catalan coastal stations, 2002/2003

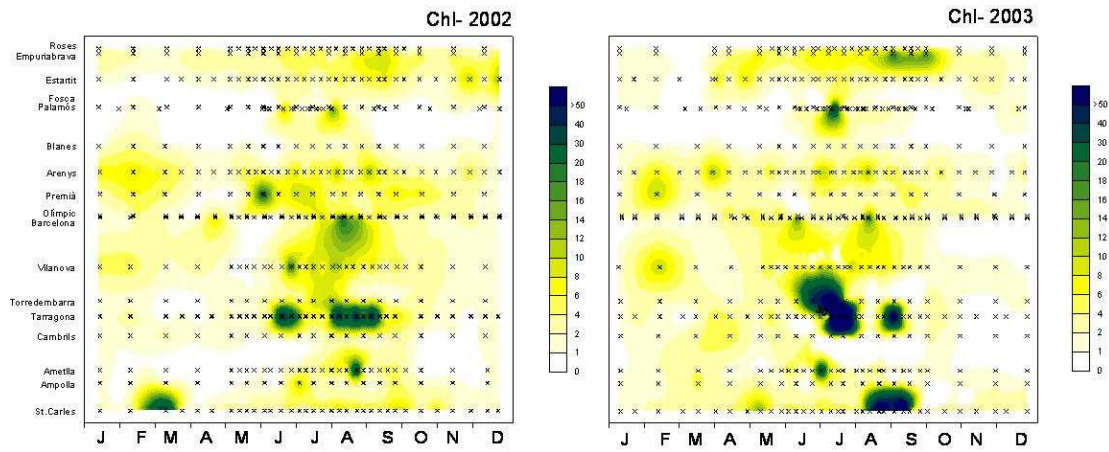




Plate A4. *Alexandrium* blooms, Catalan coastal stations, 2002/2003

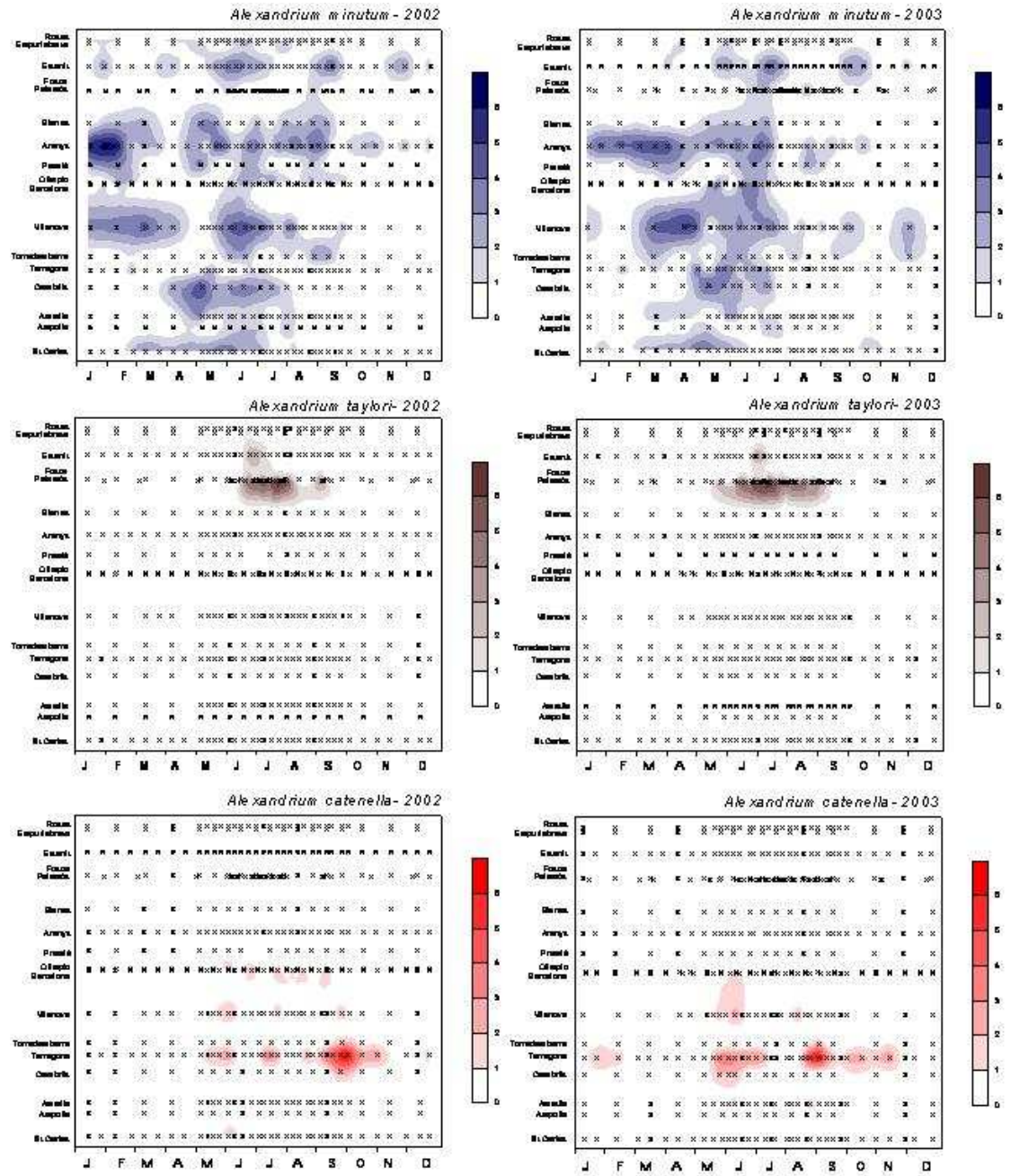
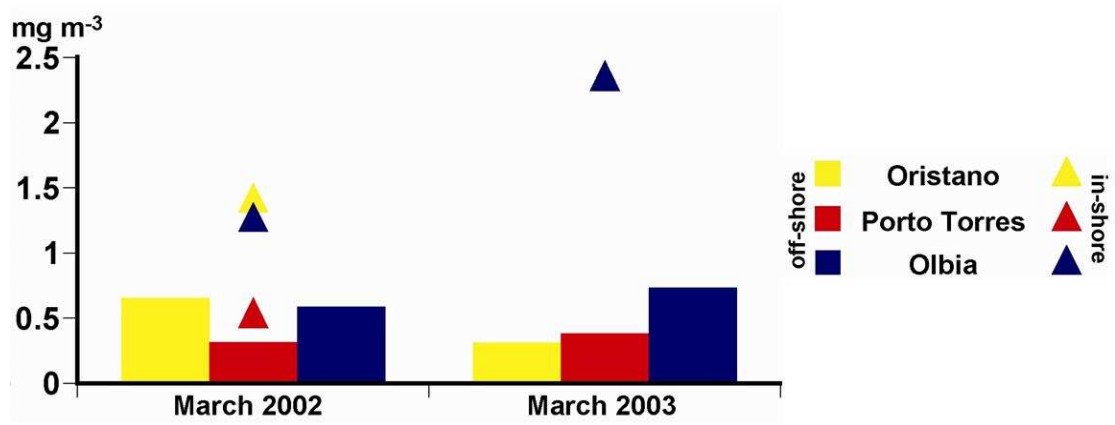




Plate A5. Total chlorophyll-a, Sardinia coastal stations, March 02/03

---





## **Mission of the JRC**

The mission of the JRC is to provide customer-driven scientific and technical support for the conception, development, implementation and monitoring of EU policies. As a service of the European Commission, the JRC functions as a reference centre of science and technology for the Union. Close to the policy-making process, it serves the common interest of the Member States, while being independent of special interests, whether private or national.

